Smart Structures and Systems, *Vol. 25, No. 1 (2020) 1-22*
DOI: https://doi.org/10.12989/sss.2020.25.1.001

A modified index for damage detection of structures using improved reduction system method

Shahin Lale Arefi [1a], Amin Gholizad*[1] and Seyed Mohammad Seyedpoor [2b]

[1] *Department of Civil Engineering, University of Mohaghegh Ardabili, P.O. Box 56199-11397, Ardabil, Iran*
[2] *Department of Civil Engineering, Shomal University, Amol, Iran*

(*Received July 28, 2018, Revised June 1, 2019, Accepted Septebmer 14, 2019*)

Abstract. The modal strain energy method is one of the efficient methods for detecting damage in the structures. Due to existing some limitations in real-world structures, sensors can only be located on a limited number of degrees of freedom (DOFs) of a structure. Therefore, the mode shape values in all DOFs of structures cannot be measured. In this paper, a modified modal strain energy based index (MMSEBI) is introduced to locate damaged elements of structures when a limited number of sensors are used. The proposed MMSEBI is based on the reconstruction of mode shapes using Improved Reduction System (IRS) method. Therefore, in the first step by employing IRS method, mode shapes in slave degrees of freedom are estimated by those of master degrees of freedom. In the second step, the proposed MMSEBI is used to located damage elements. In order to evaluate the efficiency of the proposed method, two numerical examples are considered under different damage patterns considering the measurement noise. Moreover, the universal threshold based on statistical hypothesis testing principles is applied to damage index values. The results show the effectiveness of the proposed MMSEBI for the structural damage localization when comparing with the available damage index named MESBI. The results demonstrate that the presented method can be used as a practical strategy for structural damage identification, especially when a limited number of sensors are installed on the structure. Finally, the combination of MMSEBI and IRS method can provide a reliable tool to identify the location of damage accurately.

Keywords: damage detection; modal strain energy; degrees of freedom; IRS method

1. Introduction

Nowadays, with the rapid development of science and technology, many engineering structures and imperative infrastructures have been constructed. These structures may be affected by excessive applications and natural disaster risks during their lifetime, resulting in the structural integrity will decrease. The health monitoring of a structure is a major factor in assessing damage occurrence and determining the location and the severity of possible damages (Dongyu *et al*. 2010). Damage usually alters physical properties of structures leading to decreasing the structural stiffness, but the structural mass can be assumed to be constant because of its negligible change. In addition, a change in the stiffness will modify dynamic properties of structures including natural frequencies and mode shapes (Hu and Wu 2009).

In most recent studies, mode shapes have then been utilized, due to numerous reasons, to identify the structural damage instead of natural frequencies (Guo and Li 2009, Shih *et al*. 2009, Yazdanpanah *et al*. 2015). In this regard, several techniques have been developed to detect structural damage relied on mode shapes. The modal strain energy (MSE) is one of the most efficient methods which can be used as an indicator in the structural damage detection. Due to damage occurrence and sensitivity of the mode shapes to changes in the structural properties, the strain energy changes. Thus, damage location can be identified using an efficient MSE change. The basic formulation of the MSE method is such that it requires mode shapes at all degrees of freedom. In some researches, complete degrees of freedom have been used to determine MSE of the structure, and in some others, incomplete degrees of freedom have been considered.

In recent years, much research has been carried out on the implementation of modal strain energy to detect the structural damage. Stubbs *et al*. (1992) recommended the main idea of such method. They found that MSE, defined on the basis of mode shape curvature, will change due to damage. Furthermore, they expanded their introduced method for the damage identification of structures (Stubbs *et al*. 1995). Shi *et al*. (2000a) obtained structural damage using MSE change before and after damage.

The performance of the introduced index was then elucidated through damage identification results. Kim *et al*. (2003) carried out some examinations using structural frequency responses, mode shapes and MSE so as to detect damage in structures. The results revealed that MSE is extremely sensitive to damage compared to other dynamic responses. Shi *et al*. (2002) presented a method on basis of modified modal strain energy. A two-story steel frame was

*Corresponding author, Associate Professor,
E-mail: gholizad@uma.ac.ir
[a] Ph.D. Candidate, E-mail: shahin.arefi@gmail.com
[b] Ph.D., Associate Professor,
E-mail: s.m.seyedpoor@shomal.ac.ir

http://www.techno-press.org/?journal=sss&subpage=7 ISSN: 1738-1584 (Print), 1738-1991 (Online)

adopted to illustrate the effectiveness of the proposed method. The outcomes confirmed the good performance of the method in identifying the structural damage. Moreover, an improved damage detection method based on the concept of modal strain damage index was presented by Guan and Karbhari (2008). The proposed damage index was possible to calculate modal displacements and modal rotations. A penalty-based minimization approach was then used to find the unknown modal rotation using sparse and noisy modal displacement measurement. The results indicated the advantages of the method compared to the modal curvature method. Asgarian *et al*. (2009) identified damage in jacket-type offshore platforms using MSE method. Numerous examples were then practiced to prove the efficiency of the proposed method in the identification of damage. Hu and Wu (2009) introduced a damage index for detecting damage in plates using the MSE method. such damage index was defined as a ratio of MSE before and after the damage incidence. Seyedpoor (2012) recommended a damage indicator based on MSE, and the high performance of which was assessed by some numerical examples.

Yan *et al*. (2012) formulated a damage detection method based on the elemental MSE sensitivity. The method was numerically applied to a number of two-dimensional structures and high efficiency results were then noted. Wahalthantri *et al*. (2012) investigated a damage index regarding MSE method for a simply-supported double-span beam. They proved that the method is efficient enough, though applicable only for simple beams. Ding *et al*. (2013) proposed a damage index based on MSE method for roads and bridge structures. Numerically applying the method to a bridge using a continuous beam model, good agreement was obtained by assuming various quantities of damage at different locations.

Wang *et al*. (2013) used cross modal strain energy (CMSE) method in the estimation of semi-rigid joints. In their study, a four-story frame was considered to demonstrate the capability of the presented method. It was conducted that the CMSE method can estimate the connection stiffness. Liu *et al*. (2014) conducted an experiment of improved strain energy method to identify damage in jacket-type offshore wind turbines. The experimental results demonstrated that the proposed method can properly identify the location of damage through utilizing the first two measured modes for different damage scenarios. Li *et al*. (2015) developed a damage detection method based on MSE and artificial neural networks in beams. The result showed that the method can correctly detect the damage in beams. Moradipour *et al*. (2015) used an improved MSE to identify damage in 2D structures. They mathematically developed the MSE method and then applied it to a beam and a two-dimensional frame so as to establish the efficiency of the method. The results revealed that the proposed method could be a reliable approach in detecting damage, considering 5 modes of the structure. Wu *et al*. (2016) identified damage in structures via MSE method rather addressing strain modes than displacement and rotation modes. The method was introduced on an Euler–Bernoulli beam with a uniform cross section and the outcomes verified the accuracy of the method in identifying damage. Li *et al*. (2016) proposed an improved MSE method to assess damage in offshore platform structures. To illustrate the efficiency of such method, both numerical and experimental studies were conducted for different damage cases utilizing a jacket platform structure. The results demonstrated the satisfactory performance of the method introduced for damage assessment.

Tan *et al*. (2017) could identify damage in steel beams by means of MSE method combined with artificial neural network. Some numerical examples were then used to assess the performance of the method. The results confirmed the method's high efficiency. Ashory *et al*. (2018) obtained damage in laminated composite plates using an efficient MSE. It was witnessed that damage identification using the MSE method in composite plates has acceptable results and hence the accuracy of the method is improved compared to other methods.

As yet, mode shape values at all DOFs of structures were required to evaluate MSE in many of the previous works. However, this is impossible for a real-life structure since the sensors can only be located on a limited number of DOFs of the structure. Hence, it would be quite advantageous to use a method in estimating the structural responses at all DOFs based on a limited number of DOFs and thus reduce the number of DOFs. Moreover, it seems essential to introduce a more powerful index that can efficiently and accurately detect the location of damage.

This study aims to provide a modified modal strain energy-based index (MMSEBI) to overcome the limitations of the earlier damage indicators. To achieve this goal, improved reduction system (IRS) method is employed to estimate the slave DOF responses using those of master DOFs. Then, a damage indicator is introduced to identify the damage location properly through a limited number of structural responses. The proposed method is numerically applied to a couple of examples. Single and multiple damage scenarios with 3% and 7% noise are considered and the results are compared with a previous MSE based method (Seyedpoor 2012). The outcomes of numerical studies point out the effectiveness of the suggested method.

2. Model reduction

The basis of reduction methods for decreasing the degrees of freedom (DOFs) of a structure was first introduced by Guyan (1985). In these methods, the total DOFs of a structure are divided into masters and slaves. Only master DOFs are used in a dynamic analysis, while assuming that the responses at the slave DOFs are not available. Hence, by a transmission matrix; the slave DOF responses are estimated utilizing the responses from the master DOFs, and the approximate responses will be used in the analysis process. In this section, the Guyan reduction method is expressed at first, and then the improved reduction system (IRS) method used in this study is briefly described (O'Callahan 1989). The dynamic equation of motion in a structure with n degrees of freedom can be defined as

$$[M]\{\ddot{\vec{x}}\} + [K]\{\vec{x}\} = \{\vec{f}\} \tag{1}$$

where K, M, and f are the stiffness matrix, mass matrix and the dynamic force vector, respectively.

When the total DOFs of the structure are written according to the master and slave DOFs and no force is exerted to the slave degrees of freedom, the equation of motion can be parted as

$$\begin{bmatrix}[M_{mm}] & [M_{ms}] \\ [M_{sm}] & [M_{ss}]\end{bmatrix}\begin{Bmatrix}\ddot{\vec{x}}_m \\ \ddot{\vec{x}}_s\end{Bmatrix} + \begin{bmatrix}[K_{mm}] & [K_{ms}] \\ [K_{sm}] & [K_{ss}]\end{bmatrix}\begin{Bmatrix}\vec{x}_m \\ \vec{x}_s\end{Bmatrix} = \begin{Bmatrix}\vec{f}_m \\ \vec{0}\end{Bmatrix} \tag{2}$$

where the symbols m and s denote the master and slave coordinates, respectively.

The second set of Eq. (2) by ignoring the inertia terms can be written as

$$[K_{sm}]\{\vec{x}_m\} + [K_{ss}]\{\vec{x}_s\} = 0 \tag{3}$$

Eq. (3) can be solved for slave DOFs as

$$\{\vec{x}_s\} = -[K^{-1}{}_{ss}]\,[K_{sm}]\{\vec{x}_m\} \tag{4}$$

From Eq. (4), the relation between the master and slave DOF responses is obtained where the transformation matrix T_s can be defined as

$$[T_s] = \begin{bmatrix}[I] \\ -[K_{ss}]^{-1}[K_{sm}]\end{bmatrix} \tag{5}$$

Accordingly, the reduced stiffness and mass matrices can be obtained from the following equations

$$[M_r] = [T_s]^T[M][T_s] \tag{6}$$

$$[K_r] = [T_s]^T[K][T_s] \tag{7}$$

The IRS method is an improvement of the Guyan reduction method that the mass effects on DOFs will be considered. Hence, the use of IRS instead of Guyan reduction can be expected to improve the performance of the method (O'Callahan 1989). In the IRS method, for estimating the slave DOFs from the master DOFs, the transformation matrix T_{IRS} is used instead of T_s as below

$$[T_{IRS}] = [\mathrm{T_s}] + [\mathrm{S}][\mathrm{M}][\mathrm{T_s}][M_r]^{-1}[K_r] \tag{8}$$

where the matrix S is defined as

$$S = \begin{bmatrix}0 & 0 \\ 0 & [K_{ss}^{-1}]\end{bmatrix} \tag{9}$$

Accordingly, the reduced mass and stiffness matrices (M_{IRS} and K_{IRS}, respectively) are attained as

$$[M_{IRS}] = [T_{IRS}]^T[M][T_{IRS}] \tag{10}$$

$$[K_{IRS}] = [T_{IRS}]^T[K][T_{IRS}] \tag{11}$$

Now, the mode shapes at all DOFs $\{\varphi_T\}$ using mode shapes at master DOFs $\{\varphi_m\}$, can be obtained as

$$\{\varphi_T\} = \begin{bmatrix}I \\ T_{IRS}\end{bmatrix}\{\varphi_m\} \tag{12}$$

3. Modal strain energy based index

The modal strain energy (MSE) is basically the elastic energy stored in structural elements caused by deformations due to free vibration (mode shapes) of a structure (Shi *et al*. 1998). Because of damage occurrence, the MSE alters obviously and therefore an MSE-based index can be used as an efficient way to identify damage in structures. In order to obtain the MSE, modal analysis is needed to be performed. It is a tool to determine the natural frequencies and mode shapes of a structure which is expressed as (Seyedpoor 2012)

$$([K] - \omega_{\mathrm{i}}^2[M])\{\varphi_i\} = 0, \qquad i = 1, \dots, ndf \tag{13}$$

where K and M are the stiffness and mass matrices, respectively, ω_i is the i^{th} circular frequency and φ_i is the i^{th} mode shape vector of a structure. Also, ndf is the total active DOFs of the structure.

The MSE of the e^{th} element in the i^{th} mode of the structure can be described as follow (Seyedpoor 2012)

$$mse_i^e = \frac{1}{2}\{\varphi_i^e\}^T[k^e]\{\varphi_i^e\}, \quad i = 1, \dots, ndf, \qquad e = 1, \dots, nte \tag{14}$$

where k^e is the stiffness matrix of the eth element of the structure, φ_i^e is the vector of corresponding nodal displacements of the e^{th} element in the i^{th} mode and nte is the total number of elements

Based on Eq. (14), a modal strain energy-based index (MSEBI) was introduced to identify structural damage by Seyedpoor (2012) as

$$MSEBI^e = \max\left[0, \frac{(mnmse^e)^d - (mnmse^e)^h}{(mnmse^e)^h}\right], \quad e = 1, \dots, nte \tag{15}$$

where the efficient parameter $mnmse^e$ for a healthy element and a damaged element of the structure is represented by $(mnmse^e)^{\mathrm{h}}$ and $(mnmse^e)^{\mathrm{d}}$, respectively.

It should be noted that MSEBI requires the mode shapes at all DOFs and it has not been expressed when the sensors are located on limited DOFs. Thus, a modal strain energy based index is introduced here based on using the limited DOF responses of the structure.

4. The modified modal strain energy based index

In this section, some explanations regarding the proposed index based on MSE are provided. For the structure with ndf degrees of freedom via only Nm sensors which are located on some limited degrees of freedom, Eq. (16) is used to determine the natural frequencies and mode shapes as

$$([K_r]-\omega_i^2[M_r])\{\varphi_{mi}\}=0, \quad m=1,\dots,Nm \qquad (16)$$
$$i=1,\dots,Nmode \quad Nmode\le Nm$$

where *Nmode*, *Nm*, ω_i and φ_{mi} are the number of modes, number of master DOFs, i^{th} circular frequency and i^{th} mode shape vector of master DOFs where sensor are located, respectively. Also, K_r and M_r are the reduced stiffness and mass matrices based on the IRS method for considering the limited number of DOFs.

In order to calculate the MSE of the structure, the slave DOF responses (the sensors do not install on these DOFs) need to be determined in addition to master DOF responses where sensors are installed. By calculating the mode shape vector of master DOFs of the structure (φ_{mi}) from Eq. (16), the IRS method is employed to estimate the mode shapes corresponding to the slave DOFs (φ_{si}). The compound of two sets of vectors is arranged as the mode shapes of the whole structure (φ_{Ti}) as

$$\{\varphi_{Ti}\}_{ndf\times 1}=\begin{Bmatrix}\{\varphi_{mi}\}_{nmaster\times 1}\\ \{\varphi_{si}\}_{nslave\times 1}\end{Bmatrix} \quad i=1,\dots,Nmode \qquad (17)$$

where φ_{mi} and φsi are the mode shape vectors of master and slave DOFs, respectively and φ_{Ti} is the complete mode shape vector.

Then the modal strain energy of the e^{th} element corresponding to the i^{th} mode is obtained as

$$mmse_i^e=\frac{1}{2}\{\varphi_{Ti}^e\}^T[k^e]\{\varphi_{Ti}^e\}, \qquad (18)$$
$$i=1,\dots,Nmode, \quad e=1,\dots,nte$$

where *nte* is the number of elements. The total MSE of the i^{th} structural mode ($mmse_i$) can be determined via the sum of MSE values for all elements ($mmse_i^e$) which can be expressed as

$$mmse_i=\sum_{e=1}^{nte} mmse_i^e, \quad i=1,\dots,Nmode \qquad (19)$$

In order to achieve the desired index, it is better to normalize the $mmse_i^e$ (for each element) to the $mmse_i$ (for entire structure) as

$$nmmse_i^e=\frac{mmse_i^e}{mmse_i} \qquad (20)$$

where $nmmse_i^e$ is the normalized form of MSE of the *e*th element for the *i*th mode of the structure.

Now, by summing squared of the normalized index of the *e*th element for considering all modes, an efficient parameter can be defined as

$$snmse^e=\sum_{i=1}^{Nmode}(nmmse_i^e)^2, \qquad e=1,\dots,nte \qquad (21)$$

where $snmse^e$ is named here as the efficient parameter for *e*th element of the structure. Finally, by determining the efficient parameter $snmse^e$ for healthy and damaged elements, $(snmse^e)^h$ and $(snmse^e)^d$, respectively, an effective index is defined here to identify damaged elements. The index introduced is named as a modified modal strain energy based index (MMSEBI), which can be defined by Eq. (22)

$$MMSEBI^e=max\left[0,\frac{\left(\frac{\sqrt{(snmse^e)^d}}{Nmode}\right)-\left(\frac{\sqrt{(snmse^e)^h}}{Nmode}\right)}{\sqrt{\frac{(snmse^e)^h}{Nmode}}}\right] \qquad (22)$$
$$e=1,\dots,nte$$

It should be noted that, in a real-world structure because of the unknown damage locations, it is impossible to determine the stiffness matrix of a damaged element. Hence, the stiffness matrix of the healthy element is used for determining the $(mnmse^e)^d$. According to Eq. (22), for a healthy element the index will be zero and for a damaged element the index will be larger than zero.

In this paper, both the modal strain energy based indices (MSEBI and MMSEBI), are normalized by their maximum value. Hence, MMSEBI is normalized as

$$nMMSEBI^e=\frac{MMSEBI^e}{[\max(MMSEBI)]} \qquad (23)$$

where, max(MMSEBI) is the maximum of MMSEBI in all elements.

In order to simulate damage at each element of the structure, the modulus of elasticity of each element is reduced from the original value using the following equation (Alves *et al*. 2000)

$$E_e^d=(1-\beta_e)\ E_e^h \qquad (24)$$

where E_e^d is the modulus of elasticity of the e^{th} damaged element, β_e is damage ratio of e^{th} element and E_e^h is the modulus of elasticity of the e^{th} healthy element.

5. Numerical examples

In order to assess the effectiveness of the proposed method for damage detection, two numerical examples are considered. The first example is a 45-element planar frame and the second example is a 36-bar spatial truss. In the examples, three different cases of damage are considered. Both MMSEBI and MSEBI are used to identify structural damage. The effects of mode number and noise level on the performance of the proposed method are also studied.

5.1 A forty-five-planar frame

The five-story planar frame (Kaveh *et al*. 2014) shown in Fig. 1 is considered as the first test example to assess the performance of the proposed damage index. The total number of elements and nodes is 45 and 30, respectively, leading to 75 active DOFs. All members are made of steel

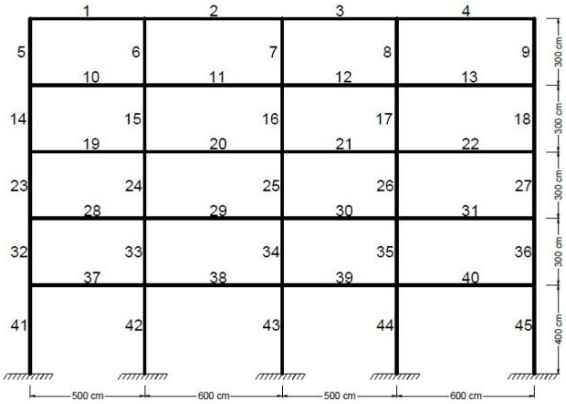

Fig. 1 A forty-five planar frame

Table 1 Different damage scenarios for the forty-five planar frame

Damage scenarios	Element number	Damage ratio
Scenario 1	43	0.30
Scenario 2	10	0.25
	32	0.30
Scenario 3	9	0.30
	18	0.20
	36	0.25

Table 2 The placement of master DOFs for the forty-five planar frame

Patterns	Master DOFs (node number/direction)							
MDOF Pattern 1	2y	3x	3y	5x	8x	10x	11x	12x
	11y	12y	20x	24x	26x	26y	30x	30y
MDOF Pattern 2	2x	2y	5x	5y	6x	6y	11x	11y
	17y	18y	26x	26y	28x	28y	30x	30y

that the elastic modulus and material density are 210 GPa and 7780 Kg/m^3, respectively. In addition, the column and beam sections are selected from W45×145 and W12×87, respectively.

Three different scenarios listed in Table 1 are utilized to investigate the performance of the proposed damage index. Two different patterns have been used for master DOFs to show the robustness of the proposed MSE-based index for damage identification. The master DOF patterns are provided in Table 2. Sixteen DOFs are selected in different nodes for each pattern, which the node number of master DOFs and its direction are given in the table.

In this paper, a universal threshold is applied to damage index values (MSEBI and MMSEBI) for every damage case. The universal threshold is defined as (Janeliukstis *et al*. 2017)

$$T = \sigma\sqrt{2\ln(I)} \tag{25}$$

where I in our case is the total number of data points and σ is the standard deviation of damage index values.

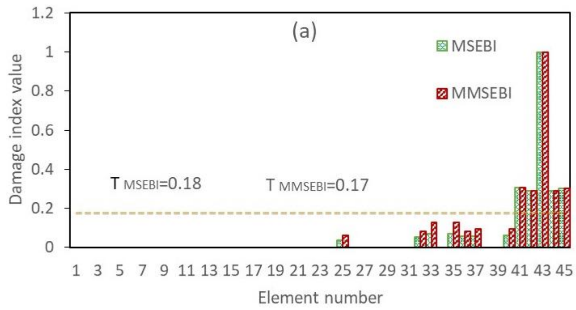

(a) Scenario 1 (damaged element: 43)

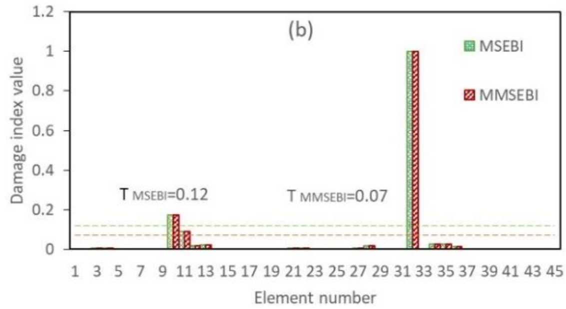

(b) Scenario 2 (damaged elements: 10, 32)

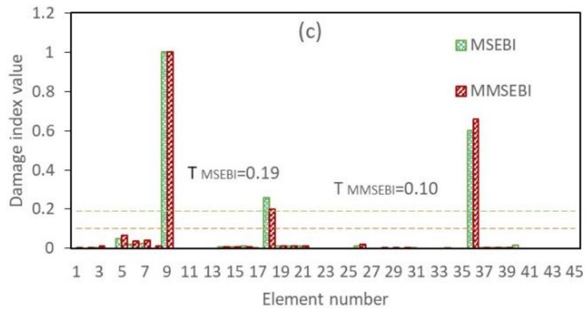

(c) Scenario 3 (damaged elements: 9, 18, 36)

Fig. 2 The normalized MSEBI and MMSEBI comparison for the 45-element planar frame for sensor pattern 1 considering 3 modes without noise

For all scenarios, elements with the index values greater than threshold value T, are considered as damaged elements. It should be noted that the index values less than the threshold value have been ignored.

Fig. 2 shows the normalized MSEBI and MMSEBI values for the first pattern of master DOFs considering 3 modes without noise. For the first damage scenario, the MSEBI and MMSEBI correctly identified the damaged element 43. However, the healthy elements 41, 42 and 44 have been detected as damaged elements.

In the second scenario, the MSEBI and MMSEBI have identified damaged elements 10 and 32. However, the MMSEBI has incorrectly identified one healthy element.

For the third scenario, the location of damaged elements 9, 18 and 36 has been accurately recognized by both indices.

In order to show the effect of mode numbers on the accuracy of the indices, the results of two damage indicators with increasing modes are also presented. Fig. 3 shows normalized MSEBI and MMSEBI values considering 5 modes for the first pattern of master DOFs without

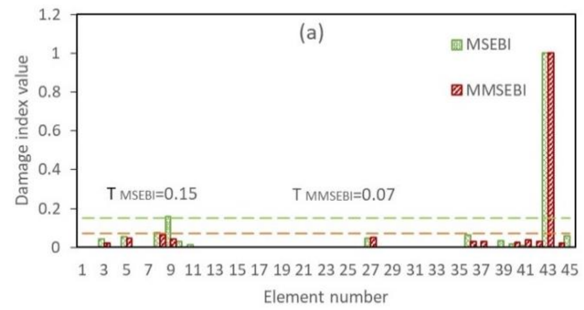

(a) Scenario 1 (damaged element: 43)

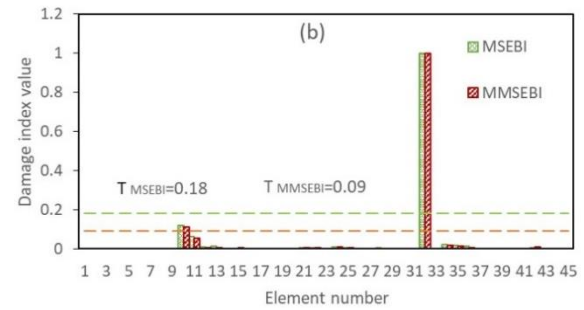

(b) Scenario 2 (damaged elements: 10, 32)

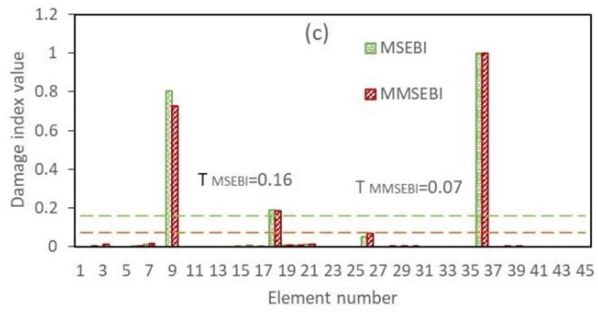

(c) Scenario 3 (damaged elements: 9, 18, 36)

Fig. 3 The normalized MSEBI and MMSEBI comparison for the 45-element planar frame for sensor pattern 1 considering 5 modes without noise

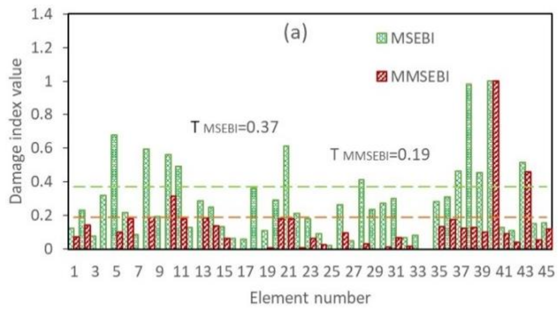

(a) Scenario 1 (damaged element: 43)

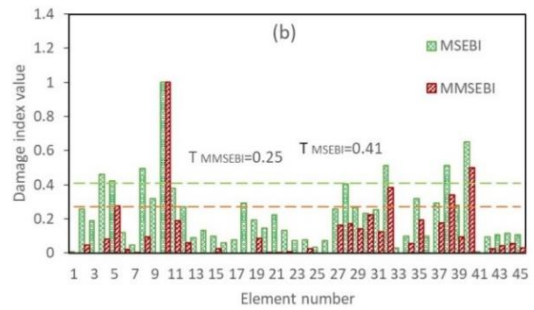

(b) Scenario 2 (damaged elements: 10, 32)

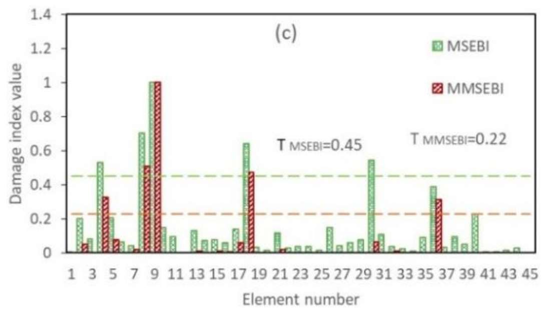

(c) Scenario 3 (damaged elements: 9, 18, 36)

Fig. 4 The normalized MSEBI and MMSEBI comparison for the 45-element planar frame for sensor pattern 1 considering 5 modes with 3% noise

considering the noise effect. As can be seen, in all three damage scenarios, the MMSEBI has properly detected damaged elements, and it has performed very well.

In order to consider the noise effect on the performance of the method, noise levels ±3% and ±7% are used in all damage scenarios applying to the mode shapes (Dinh-Cong *et al*. 2017)

$$\varphi_i^n = \varphi_i(1 + n\beta_i) \tag{26}$$

in which φ_i^n is the i*th* noisy mode shape of the structure, φ_i is i*th* mode shape of structure, n is the noise level, and β_i is a random value between [-1 1]. It has been reported that the noise levels of 2%, 3%, 5% and 7% are reasonable for mode shapes (Shi *et al*. 2000a, b, Nguyen *et al*. 2016).

With considering noise, the number of modes shapes needs to be increased in the method. Hence, 5 and 7 modes are utilized for considering the noise.

Fig. 4 demonstrates the normalized MSEBI and MMSEBI values for the first pattern of master DOFs when 5 modes with 3% noise are considered. For the first damage scenario, the MSEBI includes too many false elements where almost 10 elements are wrongly identified as damaged elements which show the low efficiency of the index. Nonetheless, the MMSEBI index has been correctly detected the location of damage just with two false elements. Therefore, the MMSEBI has a much better performance than the MSEBI. For the second scenario, the MSEBI detected about 4 elements as damaged ones. In contrast, the MMSEBI could correctly identify the exact location of damage with only two false elements. It is obvious that the MMSEBI has shown a high efficiency for detecting damage compared with the MSEBI.

In the third scenario, the MSEBI had one false element but element 36 has incorrectly identified as a healthy element. In contrast, the MMESBI showed a better accuracy while only two elements have wrongly detected. Hence, it can be said that the accuracy of the modified index for damage localization is superior.

In order to achieve the effect of the mode number, the results related to MSEBI and MMSEBI for considering more mode shapes are presented. The normalized MSEBI and MMSEBI for the first pattern of master DOFs

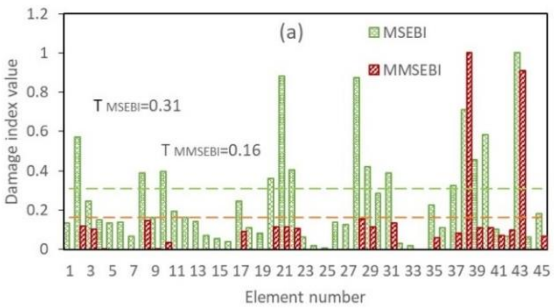

(a) Scenario 1 (damaged element: 43)

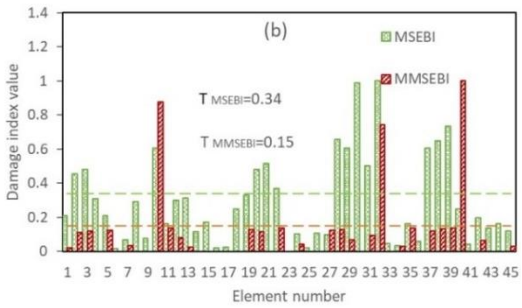

(b) Scenario 2 (damaged elements: 10, 32)

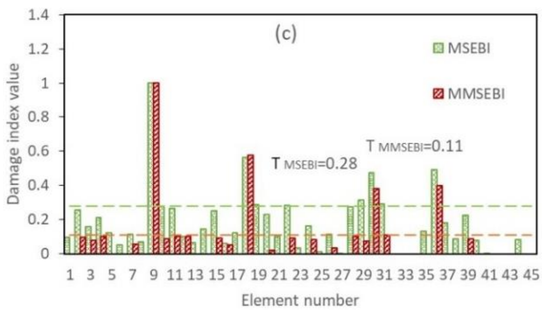

(c) Scenario 3 (damaged elements: 9, 18, 36)

Fig. 5 The normalized MSEBI and MMSEBI comparison for the 45-element planar frame for sensor pattern 1 considering 7 modes with 3% noise

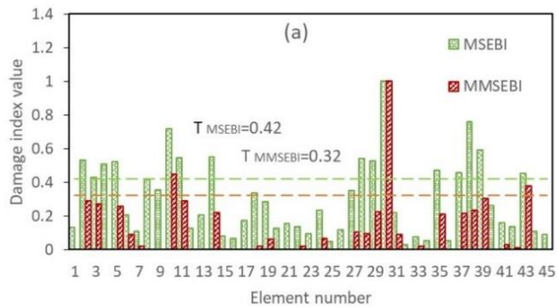

(a) Scenario 1 (damaged element: 43)

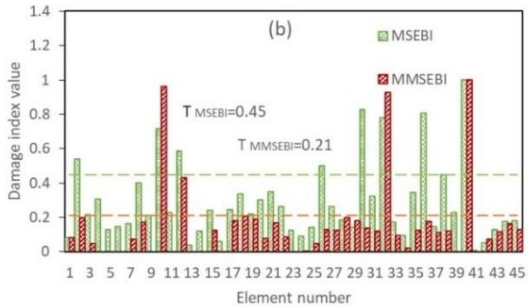

(b) Scenario 2 (damaged elements: 10, 32)

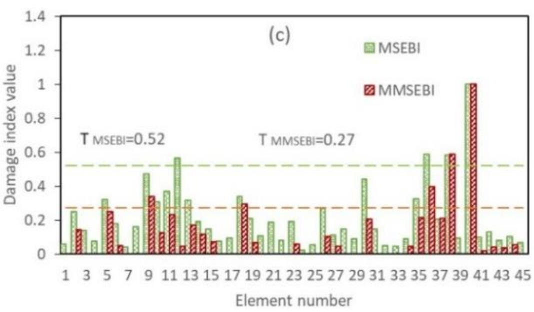

(c) Scenario 3 (damaged elements: 9, 18, 36)

Fig. 6 The normalized MSEBI and MMSEBI comparison for the 45-element planar frame for sensor pattern 1 considering 5 modes with 7% noise

considering 7 modes with 3% noise are shown in Fig. 5. It can also be noticed that the MSEBI contains a lot of false elements even by considering 7 modes. However, for all three damage scenarios, the MMSEBI could correctly identify the exact locations of damage with only one error which indicates the efficiency of the proposed index.

Fig. 6 demonstrates the normalized MSEBI and MMSEBI values for the first pattern of master DOFs when 5 modes and 7% noise are considered. For the first damage scenario, the MSEBI includes too much false elements (5, 6, 10, 11 and 23) where almost 5 elements are wrongly identified as damaged elements which show the low efficiency of the index. Nonetheless, the MMSEBI index has been correctly detected damage just with two errors. Therefore, the MMSEBI has a much better performance than the MSEBI. For the second scenario, the MSEBI detected about 7 elements (29, 30, 31, 37, 38, 39 and 40) as damaged ones. In contrast, the MMSEBI could correctly identify the exact location of damage without a false element. It is obvious that the MMSEBI has shown a high efficiency for detecting damage compared to the MSEBI.

In the third scenario, the MSEBI had 3 false elements but one damaged element 18 has incorrectly identified as a healthy element. In contrast, the MMESBI showed a better accuracy, while only three elements have wrongly detected

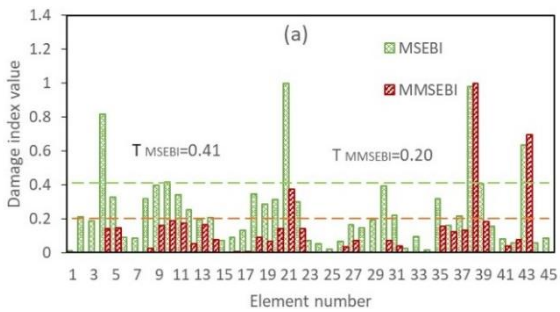

(a) Scenario 1 (damaged element: 43)

Fig. 7 The normalized MSEBI and MMSEBI comparison for the 45-element planar frame for sensor pattern 1 considering 7 modes with 7% noise

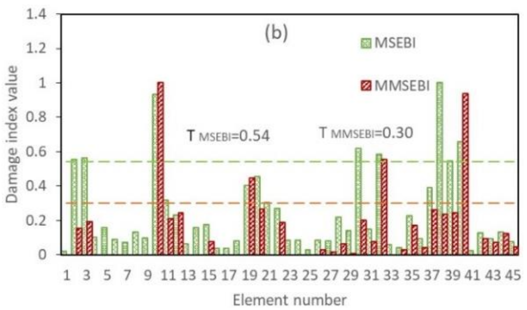

(b) Scenario 2 (damaged elements: 10, 32)

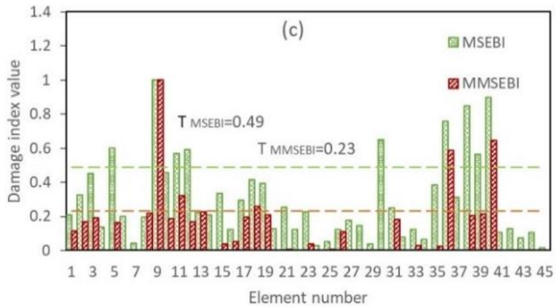

(c) Scenario 3 (damaged elements: 9, 18, 36)

Fig. 7 Continued

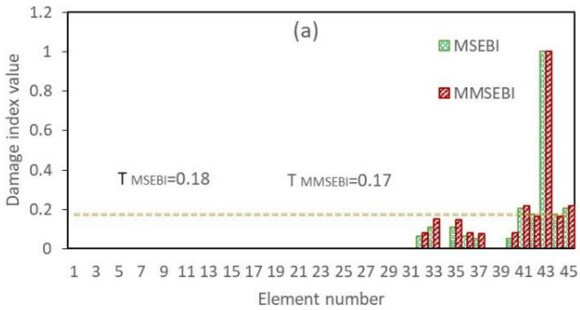

(a) Scenario 1 (damaged element: 43)

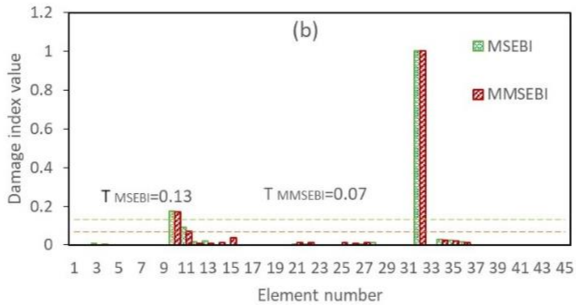

(b) Scenario 2 (damaged elements: 10, 32)

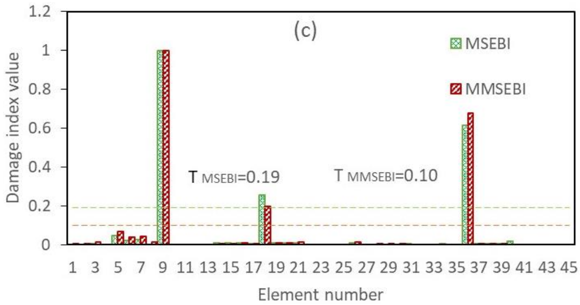

(c) Scenario 3 (damaged elements: 9, 18, 36)

Fig. 8 The normalized MSEBI and MMSEBI comparison for the 45-element planar frame for sensor pattern 2 considering 3 modes without noise

and damaged elements (9, 18 and 36) have correctly identified.

The results related to MSEBI and MMSEBI for considering more mode shapes are presented. The normalized MSEBI and MMSEBI for the first pattern of master DOFs considering 7 modes and contaminated with 7% noise are shown in Fig. 7. It can be noticed that the MSEBI contains numerous faults even by considering 7 modes. However, for all three damage scenarios, the MMSEBI could correctly identify the exact locations of damage with only two errors, indicating the efficiency of the proposed index even by increasing the noise level up to 7%.

Damage identification results of MSEBI and MMSEBI are illustrated in Fig. 8 for the second pattern of master DOFs considering 5 modes without noise. For the first damage scenario, the MSEBI and MMSEBI had similar performance and two elements 41 and 42were incorrectly identified as damaged element. Moreover, for the second damage scenario, the MSEBI and MMSEBI detected one healthy element (element 11) wrongly. Similarly, for damage scenario 3, both indices have properly recognized damaged elements 9, 18 and 36.

The MSEBI provides a higher error margin for damage scenario 3, and some elements such as elements 4, 15, 19 and 20 have also been detected as damaged wrongly. While in MMSEBI, the damaged location is correctly obtained. Consequently, the proposed index (MMSEBI) provides better performance as compared with MSEBI.

In order to demonstrate the mode numbers' effects, the results of MSEBI and MMSEBI for considering higher modes are presented. Fig. 9 displays the MSEBI and MMSEBI values for the second pattern of master DOFs considering 7 modes without noise. As can be seen for all damage scenarios, the MMSEBI index has identified damage without a false element especially in the second and third scenarios compared with the MSEBI and it performs well.

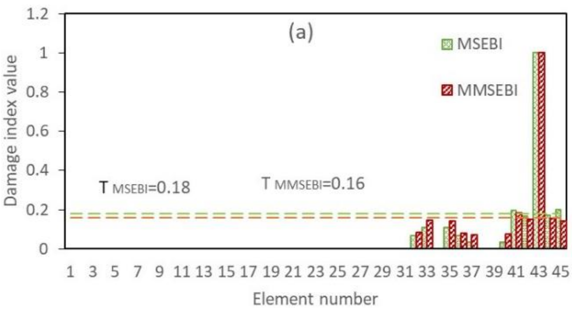

(a) Scenario 1 (damaged element: 43)

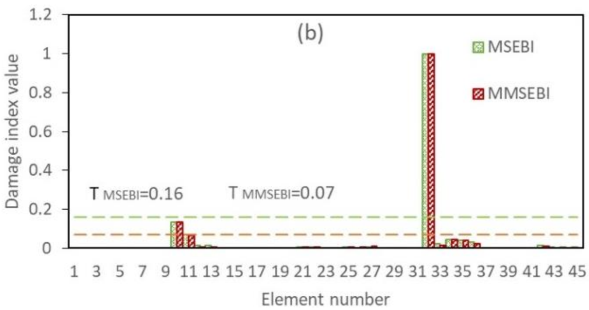

(b) Scenario 2 (damaged elements: 10, 32)

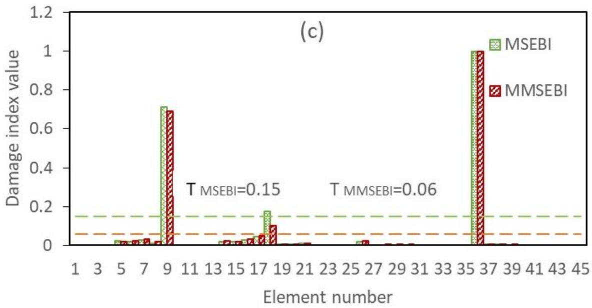

(c) Scenario 3 (damaged elements: 9, 18, 36)

Fig. 9 The normalized MSEBI and MMSEBI comparison for the 45-element planar frame for sensor pattern 2 considering 5 modes without noise

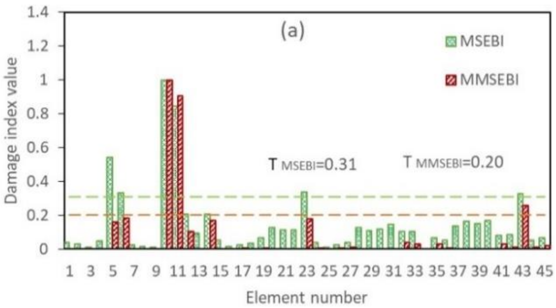

(a) Scenario 1 (damaged element: 43)

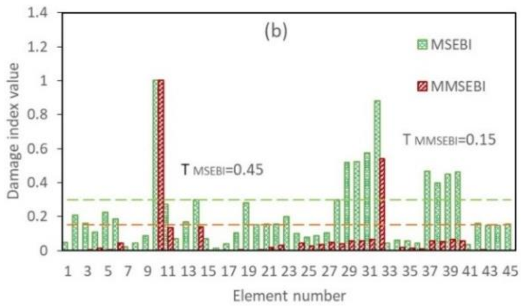

(b) Scenario 2 (damaged elements: 10, 32)

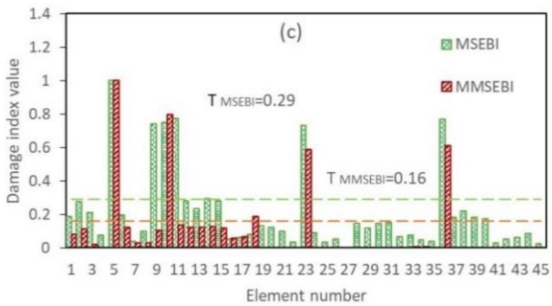

(c) Scenario 3 (damaged elements: 9, 18, 36)

Fig. 10 The normalized MSEBI and MMSEBI comparison for the 45-element planar frame for sensor pattern 2 considering 5 modes with 3% noise

Fig. 10 demonstrates the values of the normalized MSEBI and MMSEBI for the second pattern of master DOFs for considering 5 modes via 3% noise. For the first damage scenario, many errors have been seen in the MSEBI indicator where 5 elements are wrongly identified as damaged elements which show the low performance of the index. On the other hand, the MMSEBI index has been properly identified damage locations only two false elements had achieved. In the second damaged scenario, the MSEBI has incorrectly detected 7 healthy elements as damaged ones. However, the damaged elements are properly recognized by the MMSEBI indicator without a false element. In the third scenario, the MSEBI has led to lower false identification and 4 healthy elements have wrongly found as damaged elements. It means that the index does not perform well. However, the MMESBI has correctly identified damage locations only with two false elements. Consequently, it can be said that the introduced index has much better performance than the previous one.

To assess the effect of mode numbers on the efficiency of the method, the MSEBI and MMSEBI outcomes considering 7 modes are also presented. Fig. 11 demonstrates MSEBI and MMSEBI values for the second pattern of master DOFs considering 7 modes via 3% noise.

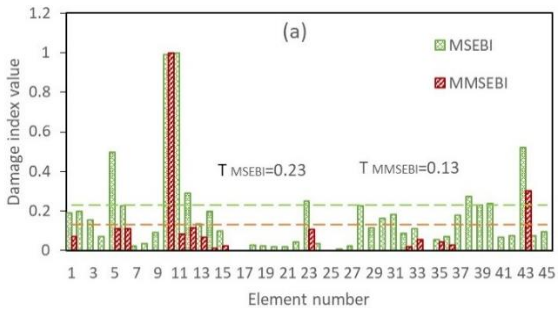

(a) Scenario 1 (damaged element: 43)

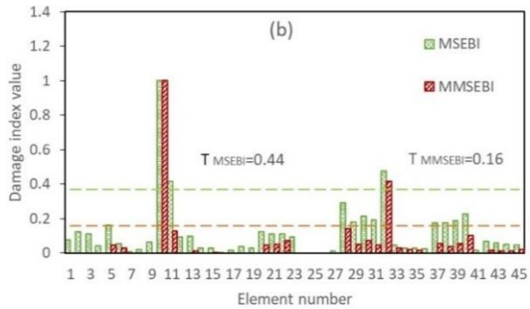

(b) Scenario 2 (damaged elements: 10, 32)

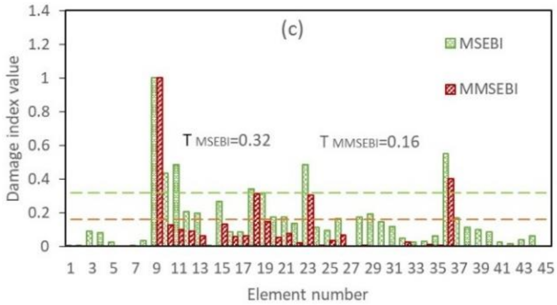

(c) Scenario 3 (damaged elements: 9, 18, 36)

Fig. 11 The normalized MSEBI and MMSEBI comparison for the 45-element planar frame for sensor pattern 2 considering 7 modes with 3% noise

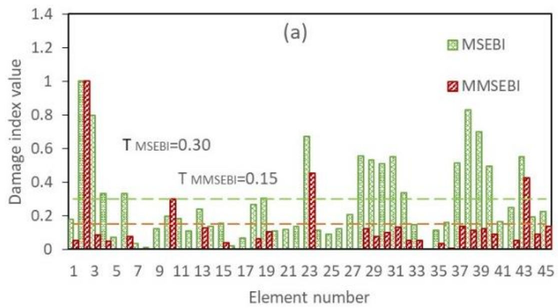

(a) Scenario 1 (damaged element: 43)

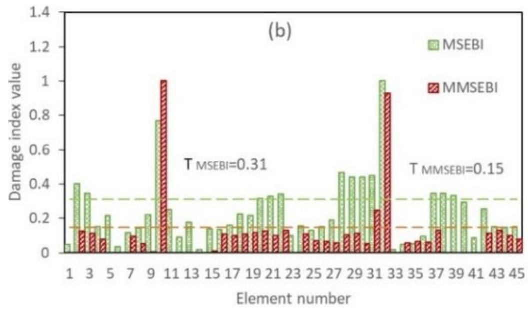

(b) Scenario 2 (damaged elements: 10, 32)

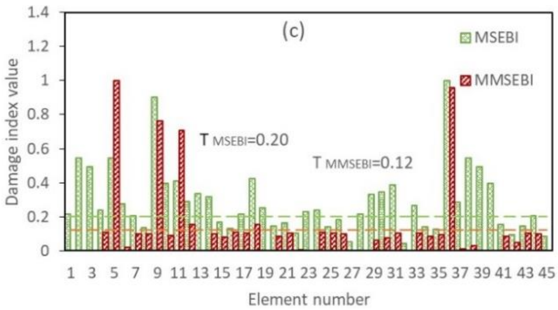

(c) Scenario 3 (damaged elements: 9, 18, 36)

Fig. 12 The normalized MSEBI and MMSEBI comparison for the 45-element planar frame for sensor pattern 2 considering 5 modes with 7% noise

It is observed from the results that the MSEBI contains a lot of false elements even by considering 7 modes. The MMSEBI index could properly identify the damage location for all damage scenarios that indicates the efficiency of the proposed index.

Fig. 12 demonstrates the normalized MSEBI and MMSEBI values for the second pattern of master DOFs when 5 modes and 7% noise are considered. For the first damage scenario, the MSEBI includes too much false elements (2, 3, 4, 6, 23, 28, 29, 30, 31, 32, 37, 38, 39 and 40) where almost 14 elements are wrongly identified as damaged elements which shows the low efficiency of the index. Nonetheless, the MMSEBI index has been correctly detected damage just with three errors. Therefore, the MMSEBI has much better performance than the MSEBI. For the second scenario, the MSEBI detected about 12 elements (2, 3, 20, 21, 22, 28, 29, 30, 31, 32, 37, 38 and 39) as damaged ones. In contrast, the MMSEBI could correctly identify the exact location of damage with only one false element. It is obvious that the MMSEBI has shown a high efficiency for detecting damage compared with the MSEBI.

In the third damage case, the MSEBI has been led to a greater error and the elements 1, 2, 3, 4, 5, 6, 7, 0, 11, 12, 13, 14, 17, 19, 23, 24, 29, 30, 31, 33, 37, 38, 39 and 40 are wrongly recognized as damaged elements. In fact, the indicator has lost its efficacy. Moreover, the damage locations have been properly identified with two errors (5, 11) by MMSEBI. Thus, it can be said that the modified index has better capability for damage identification.

The results related to the MSEBI and MMSEBI for considering more mode shapes are presented. The normalized MSEBI and MMSEBI for the second pattern of master DOFs considering 7 modes with 7% noise are shown in Fig. 13. It can also be noticed that the MSEBI contains lots of false elements even by increasing to 7 modes. However, for all three damage scenarios, the MMSEBI could correctly identify the exact locations of damage without false elements in scenarios 2 and two false elements in scenarios 1 and 3 which indicates the efficiency of the proposed index even by increasing the noise level up to 7%.

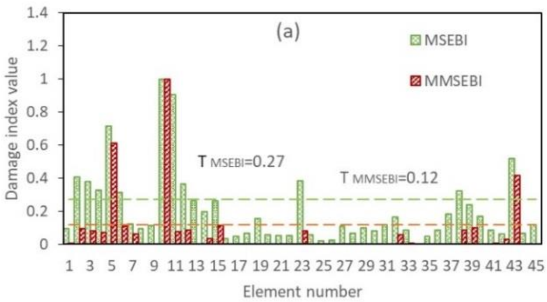

(a) Scenario 1 (damaged element: 43)

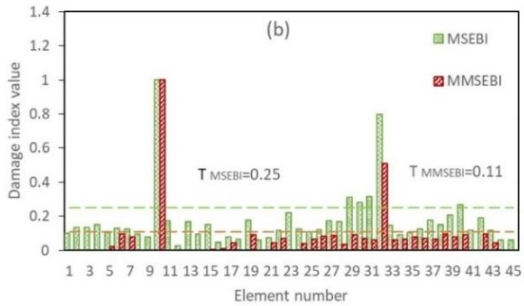

(b) Scenario 2 (damaged elements: 10, 32)

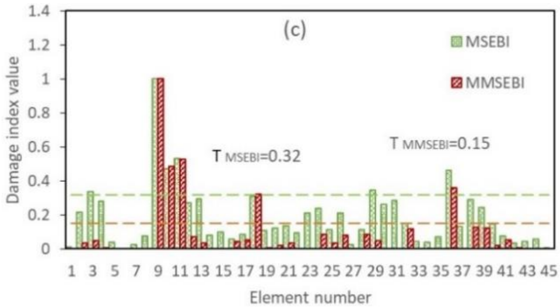

(c) Scenario 3 (damaged elements: 9, 18, 36)

Fig. 13 The normalized MSEBI and MMSEBI comparison for the 45-element planar frame for sensor pattern 2 considering 7 modes with 7% noise

Table 3 Damage elements identified for the forty-five planar frame without considering noise

Scenarios	MDOF Pattern	Actual damage	3 modes		5 modes	
			MSEBI	MMSEBI	MSEBI	MMSEBI
Scenario1		43	41, 42, 43, 44	41, 42, 43, 44	8, 43	43
Scenario2	MDOF Pattern 1	10, 32	10, 11, 32	10, 32	10, 32	10, 32
Scenario3		9, 18, 36	9, 18, 36	9, 18, 36	9, 18, 36	9, 18, 36
Scenario1		43	41, 43, 45	41, 43, 45	41, 43, 44, 45	41, 43
Scenario2	MDOF Pattern 2	10, 32	10, 11, 32	10, 11, 32	10, 32	10, 32
Scenario3		9, 18, 36	9, 18, 36	9, 18, 36	9, 18, 36	9, 18, 36

Table 4 Damage elements identified for the forty-five planar frame with considering 3% noise

Scenarios	MDOF Pattern	Actual damage	5 modes		7 modes	
			MSEBI	MMSEBI	MSEBI	MMSEBI
Scenario1	MDOF Pattern 1	43	5, 8, 10, 11, 21, 28, 37, 38, 39, 40, 43	10, 40, 43	2, 8, 10, 20, 21, 22, 28, 29, 31, 37, 38, 39, 40, 43	38, 43
Scenario2		10, 32	4, 5, 8, 32, 38, 40	10, 32, 38, 40	2, 3, 10, 20, 21, 22, 28, 29, 30, 31, 37, 38, 39	10, 32, 40
Scenario3		9, 18, 36	4, 8, 9, 18, 30, 39	4, 8, 9, 18, 36	9, 18, 29, 30, 31, 36	9, 18, 30, 36
Scenario1	MDOF Pattern 2	43	5, 6, 10, 11, 23, 43	10, 11, 43	5, 10, 11, 12, 23, 38, 40, 43	10, 43
Scenario2		10, 32	10, 29, 30, 31, 32, 37, 38, 39, 40	10, 32	10, 11, 32	10, 32
Scenario3		9, 18, 36	5, 9, 10, 11, 23, 36	5, 9, 10, 18, 23, 36	9, 10, 11, 18, 19, 23, 36	9, 18, 23, 36

Table 5 Damage elements identified for the forty-five planar frame with considering 7% noise

Scenarios	MDOF Pattern	Actual damage	5 modes		7 modes	
			MSEBI	MMSEBI	MSEBI	MMSEBI
Scenario1	MDOF Pattern 1	43	2, 8, 10, 20, 21, 22, 37, 38, 39, 40, 43	38, 43	4, 10, 21, 28, 43	38, 43
Scenario2		10, 32	2, 10, 12, 26, 30, 32, 36, 40	10, 12, 32, 40	2, 3, 10, 30, 32, 38, 39, 40	10, 20, 32, 40
Scenario3		9, 18, 36	9, 12, 18, 36, 38, 40	9, 18, 36, 38, 40	5, 9, 11, 12, 18, 30, 36, 38, 39, 40	9, 11, 18, 36, 40
Scenario1	MDOF Pattern 2	43	2, 3, 4, 6, 23, 28, 29, 30, 31, 32, 37, 38, 39, 40, 43	2, 10, 23, 43	2, 3, 4, 5, 6, 10, 11, 12, 23, 38, 43	5, 10, 43
Scenario2		10, 32	2, 3, 10, 20, 21, 22, 28, 29, 30, 31, 32, 37, 38, 39	10, 31, 32	10, 29, 30, 31, 32, 40	10, 32
Scenario3		9, 18, 36	1, 2, 3, 4, 5, 6, 7, 9, 10, 11, 12, 13, 14, 17, 18, 19, 23, 24, 29, 30, 31, 33, 36, 37, 38, 39, 40	5, 9, 11, 12, 18, 36	3, 10, 11, 12, 18, 29, 36	9, 10, 11, 18, 36

Table 3 presents a summary of the results obtained from the MSEBI and the proposed MMSEBI index without a noise level in the frame. As can be seen, the MSEBI and MMSEBI have almost similar performance in this case. Increasing the number of modes has also improved the performance of proposed MMSEBI versus MSEBI where the MMSEBI has been able to detect damage without false elements by using 7 modes. The increase in the number of modes has however minor effect on the performance of MSEBI.

Moreover, for the MSEBI, the second pattern of DOFs has a better efficiency compared with the first pattern of DOFs. Though, in both patterns, a lot of false elements has been gained. But, the use of the MMSEBI has resulted in a good performance in both patterns which damaged elements are properly identified. Both patterns have rather the similar efficiency for damage identification. However, the result showed the second pattern is better than the first one.

Table 4 summarizes the damage identification results obtained by MSEBI and MMSEBI, considering 3% of noise. As can be seen, MSEBI contains a good deal of false elements in detecting the damaged location in scenarios 1, 2 and 3. Only in scenarios 1 and 3, the MMSEBI respectively predicts elements 10, 11 and elements 5, 11 as false elements for the second pattern of DOFs. The damage location is satisfactory in the rest of scenarios. By increasing the number of modes, MMSEBI has been able to detect the damage location with only one wrong element via considering 7 modes. However, an increase in the number of modes has negligible effect on the performance of MSEBI.

Table 5 reports a summary of damage identification results obtained by MSEBI and MMSEBI with 7% of noise.

As shown, the MSEBI contains lots of false elements in detecting the damage location in scenarios 1, 2 and 3. In contrast, the MMSEBI predicts damaged elements properly with only some false elements. By increasing the number of modes, the MMSEBI has been able to detect the damage location with only one wrong element via considering 7 modes, however the increase in the number of modes has little effect on the performance of the MSEBI index. Moreover, for the MMSEBI, the second pattern of DOFs

Table 6 Different damage scenarios for the 36 bar spatial truss

Damage scenarios	Element number	Damage ratio
Scenario 1	19	0.25
Scenario 2	24	0.25
Scenario 3	19	0.25
	24	0.25

Table 7 The location of master DOFs for the 36-bar spatial truss

Pattern	Master DOFs (node number/direction)			
MDOF Pattern 1	1y	1z	3x	4x
	6x	6z	10z	12x
MDOF Pattern 2	2x	2y	3y	4z
	5z	7z	11x	12x

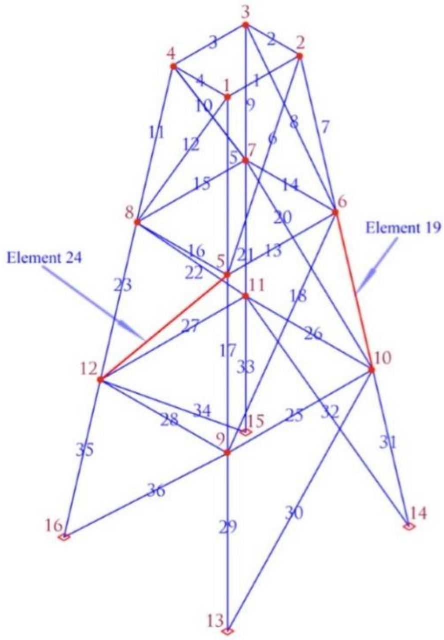

Fig. 14 The 36-bar spatial truss

has a better efficiency compared with the first pattern of DOFs. But, the use of the MSEBI has not resulted in a good performance in both damage patterns.

5.2 Thirty-six-bar spatial truss

In order to investigate the performance of the proposed method for damage detection of space trusses (3D structures), a 36-bar spatial truss shown in Fig. 14 is considered as the second example (Seyedpoor and Montazer 2016). The structure is fixed at the ground and consists of 36 steel tubular members that comprise 12 leg members, 12 horizontal members and 12 diagonal brace members in vertical planes. All members have a uniform outer diameter 17.8 cm and wall thickness 0.89 cm. The heights of all three stories are 9.14 m and the side lengths of the bottom base and top floor are 12.19 ×10.97 m and 4.88 × 3.66 m, respectively.

Each node has three degrees of freedom, so the truss structure has 36 active DOFs, and the bar element is utilized to model the truss. All members are made of steel, and the

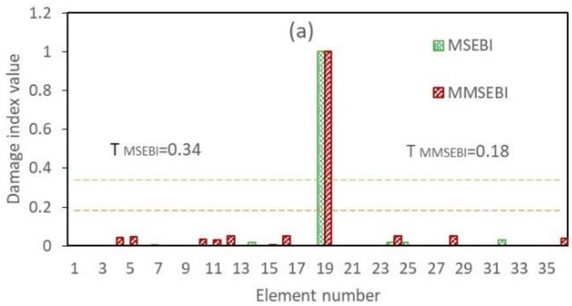

(a) Scenario 1 (damaged element: 19)

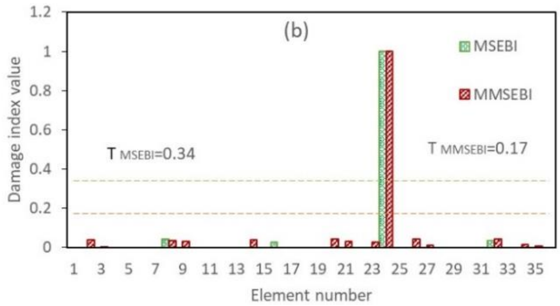

(b) Scenario 2 (damaged element: 24)

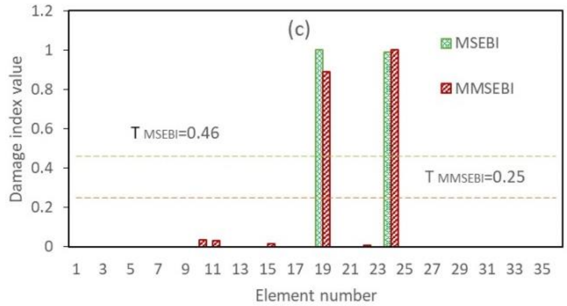

(c) Scenario 3 (damaged elements: 19, 24)

Fig. 15 The normalized MSEBI and MMSEBI comparison for the 36-bar spatial truss for sensor pattern 1 considering 3 modes without noise

Young's modulus and the mass density are 210 GPa and 7850 kg/m^3, respectively. Three different damage scenarios given in Table 6 are considered to assess the efficiency of the proposed index.

To investigate the performance of the proposed MSE-based index for damage detection, two different patterns have been used for the sensor placement. The master DOFs patterns are given in Table 7. For each pattern, 8 DOFs are selected that nodes corresponding to master DOFs and their direction are listed.

Fig. 15 compares the normalized MSEBI with the normalized MMSEBI based on the first pattern of master DOFs when 3 modes without the noise are considered.

According to the illustrated results, as for the first

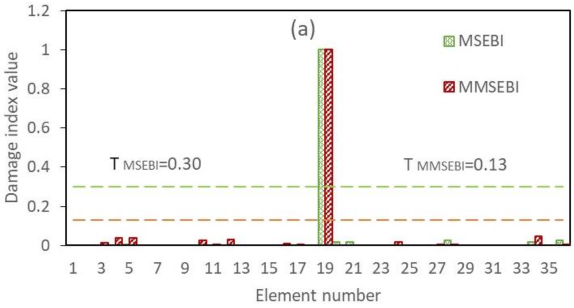

(a) Scenario 1 (damaged element: 19)

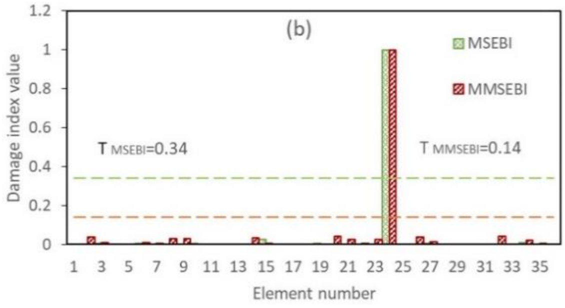

(b) Scenario 2 (damaged element: 24)

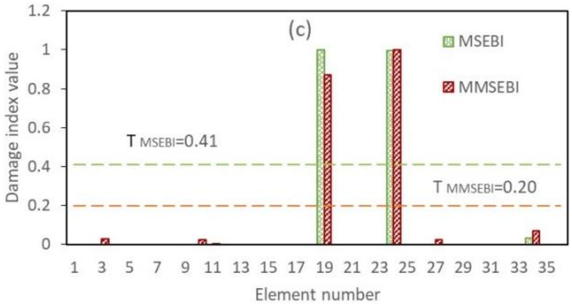

(c) Scenario 3 (damaged elements: 19, 24)

Fig. 16 The normalized MSEBI and MMSEBI comparison for the 36-bar spatial truss for sensor pattern 1 considering 4 modes without noise

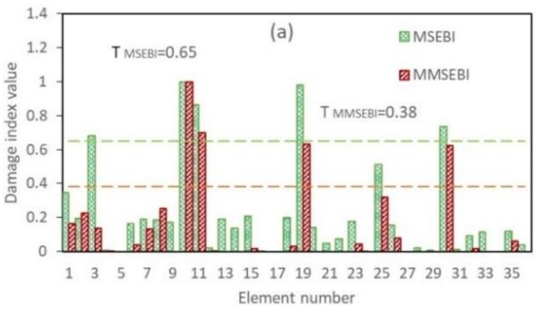

(a) Scenario 1 (damaged element: 19)

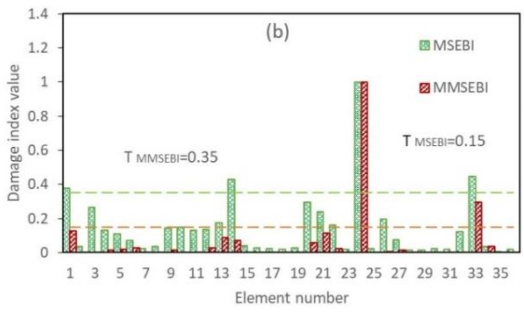

(b) Scenario 2 (damaged element: 24)

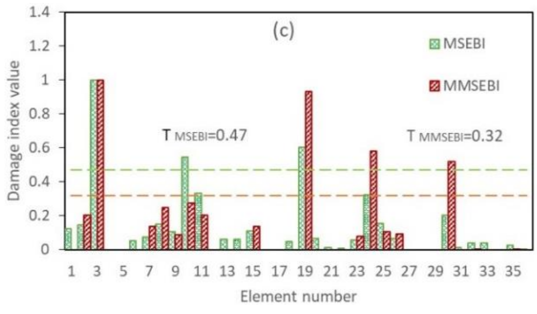

(c) Scenario 3 (damaged elements: 19, 24)

Fig. 17 The normalized MSEBI and MMSEBI comparison for the 36-bar spatial truss for sensor pattern 1 considering 5 modes with 3% noise damage scenario, both MSEBI and MMSEBI could correctly identify the damage location, and the MMSEBI value for one element (element 19) is greater than the threshold value. In the second and third damage scenarios, both MSEBI and MMSEBI can properly detect the damage location without a false element.

In order to evaluate the effect of mode numbers on the performance of two MSEBI and MMSEBI indicators, the obtained results were extended to the other modes. The MSEBI and MMSEBI values for the first pattern of master DOFs with 4 modes and without the noise effect are demonstrated in Fig. 16. The outcomes affirm that the number of damaged elements obtained with 4 modes is similar in both indices. In fact, regardless of increase in the number of mode shapes, MSEBI and MMSEBI have identical performances in damage identification.

In the case of considering the noise effect, the number of mode shapes needs to be increased. Hence, 5 and 7 modes are utilized here for considering the noise.

Fig. 17 shows the normalized MSEBI and MMSEBI values for the first pattern of master DOFs when 5 modes and 3% noise are considered. As indicated by the results, for the first damage scenario, the MSEBI contains some false elements. In addition to the damaged element 19 identified, many other elements such as 3, 10, 11 and 30 have also been wrongly detected. However, the damaged element 19 has been properly identified with only three false elements (10, 11 and 30) by MMSEBI. For the second scenario, the MSEBI recognized the damaged element 24 correctly but some healthy elements including 1, 14 and 33 are diagnosed as damaged elements. While, the MMSEBI has identified the damaged element (24) with only one false element (33). In the third damage scenario, the MSEBI has identified two false elements (3, 10). Moreover, the MSEBI has not diagnosed induced damaged element (24). In fact, the indicator has lost its efficacy. However, damage locations have been properly identified with only two errors (3, 30) by MMSEBI. Consequently, it can be said that the proposed index has a better capability for damage identification.

To assess the effect of mode numbers, the MSEBI and MMSEBI outcomes are shown in Fig. 18 for the first pattern of master DOFs considering 7 modes via 3% noise. It can be seen that the MMSEBI considering 7 modes could identify the damage locality for the third damage scenario without a false element. For the first and second damage scenarios, the MMSEBI has correctly detected the location of damages, only locating one false element. Therefore, it can point out the advantage of the index.

Fig. 19 shows the normalized MSEBI and MMSEBI values for the first pattern of master DOFs when 5 modes and 7% noise are considered. As indicated by results, for the first damage scenario, the MSEBI contains high false elements. In addition to damaged element 19 identified, other elements such as 1, 10, 11, 25 and 30 have also been wrongly detected. However, the damaged element 19 has been properly identified with three false elements (10, 11, 30) by MMSEBI. For the second scenario, the MSEBI recognized the damaged element 24 correctly but high healthy elements including 1, 3, 10, 11, 13, 14, 20, 22 and 33 are identified as damaged elements. It means, in this pattern the indicator has lost its effectiveness. While, the MMSEBI has identified the damaged elements and just two elements (13, 33) have been incorrectly detected. In the third damage case, the MSEBI has been led to a greater error and the elements 10, 11, 15 and 30 are wrongly recognized as damaged elements. Moreover, damage locations have been properly identified with two errors (25, 30) by MMSEBI. Consequently, it can be said that the

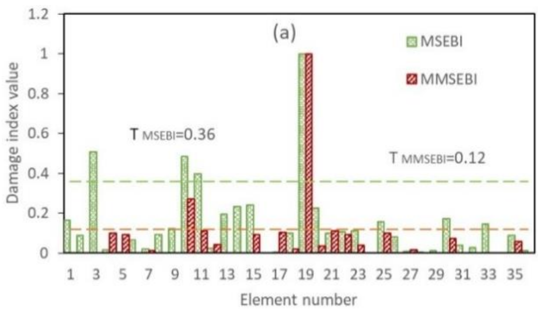

(a) Scenario 1 (damaged element: 19)

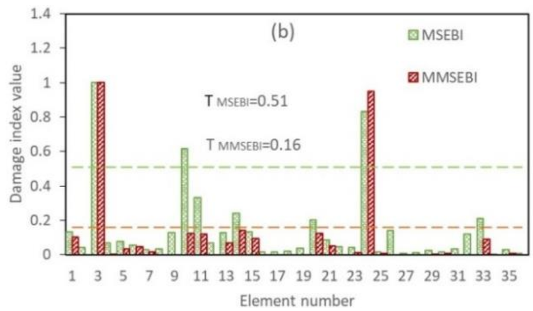

(b) Scenario 2 (damaged element: 24)

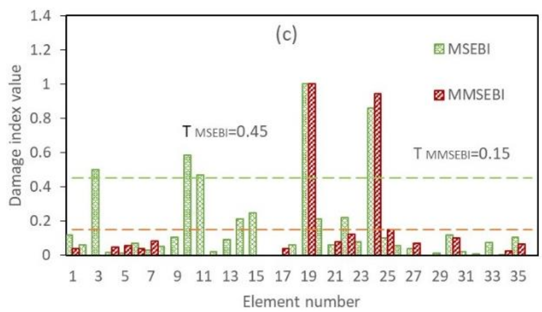

(c) Scenario 3 (damaged elements: 19, 24)

Fig. 18 The normalized MSEBI and MMSEBI comparison for the 36- bar spatial truss for sensor pattern 1 considering 7 modes with 3% noise

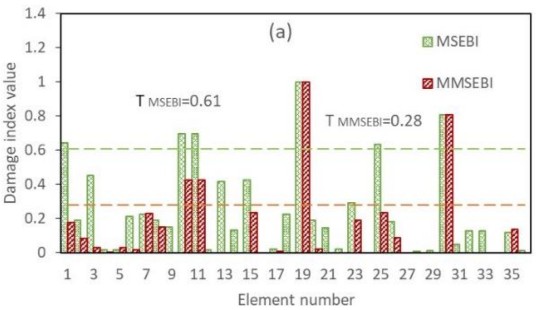

(a) Scenario 1 (damaged element: 19)

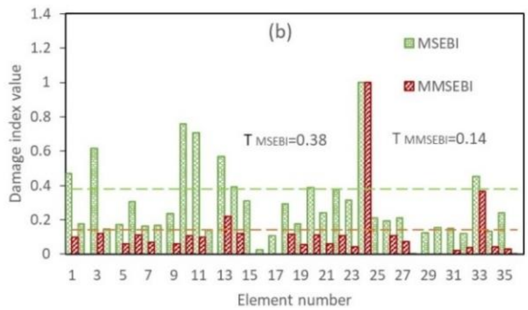

(b) Scenario 2 (damaged element: 24)

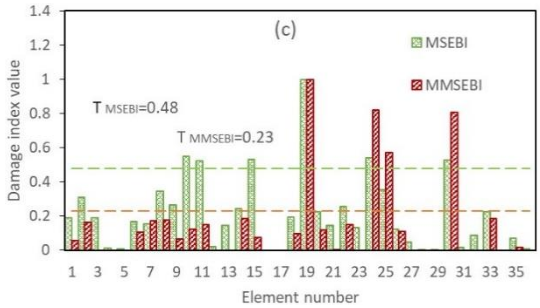

(c) Scenario 3 (damaged elements: 19, 24)

Fig. 19 The normalized MSEBI and MMSEBI comparison for the 36- bar spatial truss for sensor pattern 1 considering 5 modes with 7% noise

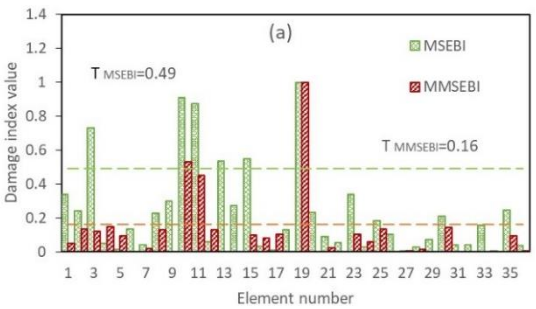

(a) Scenario 1 (damaged element: 19)

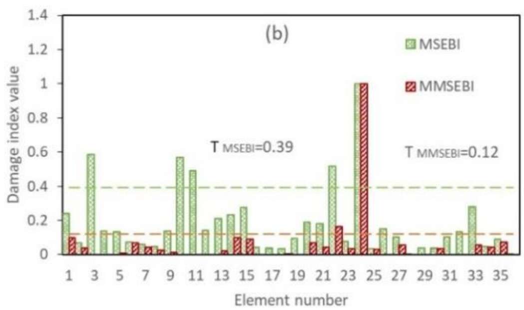

(b) Scenario 2 (damaged element: 24)

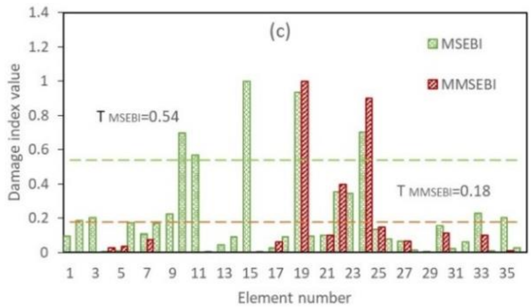

(c) Scenario 3 (damaged elements: 19, 24)

Fig. 20 The normalized MSEBI and MMSEBI comparison for the 36- bar spatial truss for sensor pattern 1 considering 7 modes with 7% noise

modified index has a better capability for damage identification even by increasing the noise level.

The normalized MSEBI and MMSEBI values are shown in Fig. 20 for considering 7 modes via 7% noise. It can be observed that the MMSEBI considering 7 modes can correctly identify the damage location for all damage scenarios with only one or two false elements, which it indicates the performance of the proposed index even by increasing the noise level.

Another sensor placement is also used to investigate the effectiveness of the indicator. Fig. 21 shows the normalized MSEBI and MMSEBI values for the second pattern of master DOFs considering 3 modes, without noise effects. The outcomes show the accuracy of both indices (MSEBI, MMSEBI) for locating the damaged element in all damage scenarios.

The results of MSEBI and MMSEBI are also presented to show the effect of the number of mode shapes. The values of MSEBI and MMSEBI for the second pattern of master DOFs using 4 modes regardless the noise effect are shown in Fig. 22. It can be seen that the MSEBI and MMSEBI have correctly identified damage locality which signifies the high performance of the proposed indicator. Consequently, despite of increasing the number of mode shapes, the MSEBI and MMSEBI have the similar performance in damage identification.

Fig. 23 demonstrates the normalized MSEBI and MMSEBI values for the second pattern of master DOFs

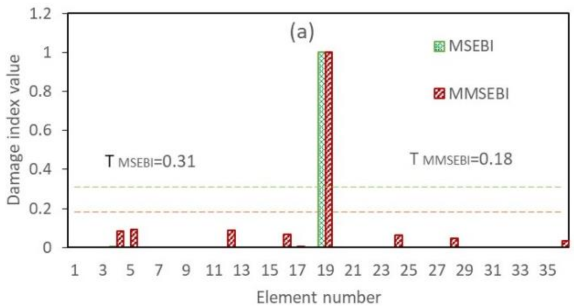

(a) Scenario 1 (damaged element: 19)

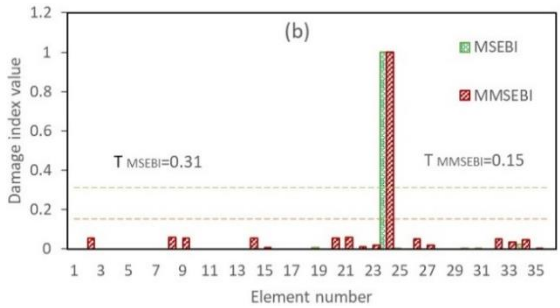

(b) Scenario 2 (damaged element: 24)

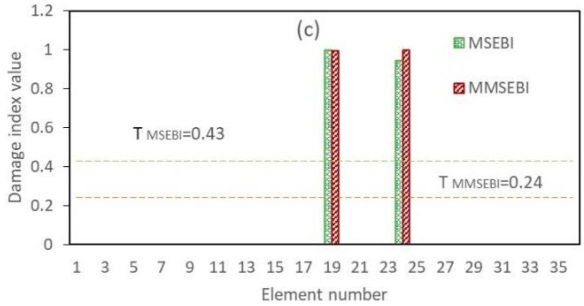

(c) Scenario 3 (damaged elements: 19, 24)

Fig. 21 The normalized MSEBI and MMSEBI comparison for the 36-bar spatial truss for sensor pattern 2 considering 3 modes without noise

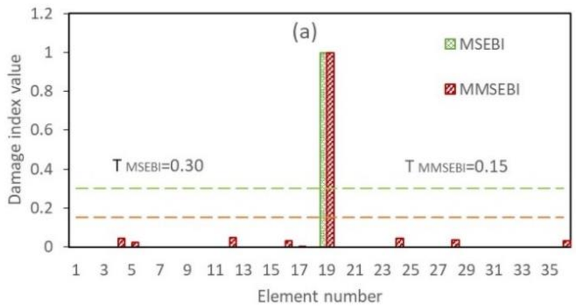

(a) Scenario 1 (damaged element: 19)

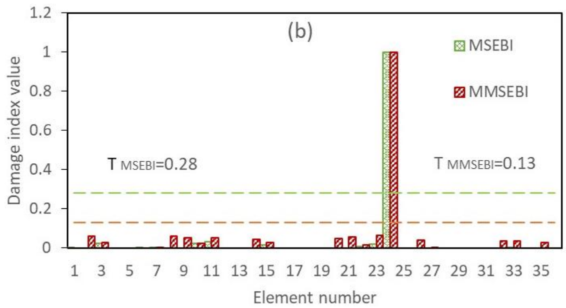

(b) Scenario 2 (damaged element: 24)

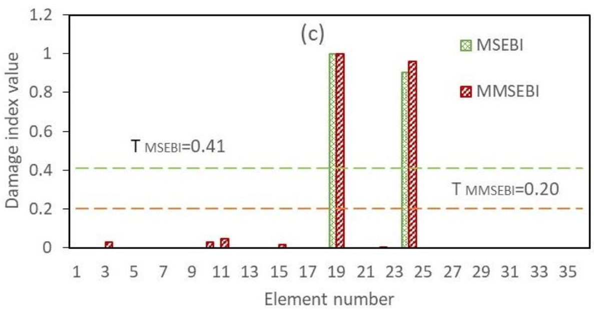

(c) Scenario 3 (damaged elements: 19, 24)

Fig. 22 The normalized MSEBI and MMSEBI comparison for the 36-bar spatial truss for sensor pattern 2 considering 4 modes without noise

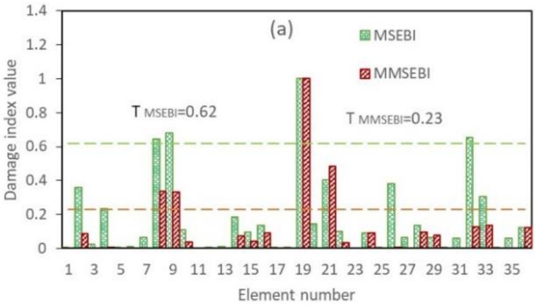

(a) Scenario 1 (damaged element: 19)

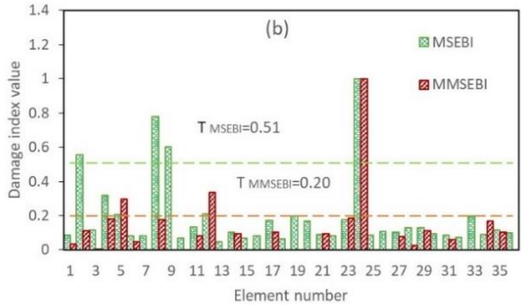

(b) Scenario 2 (damaged element: 24)

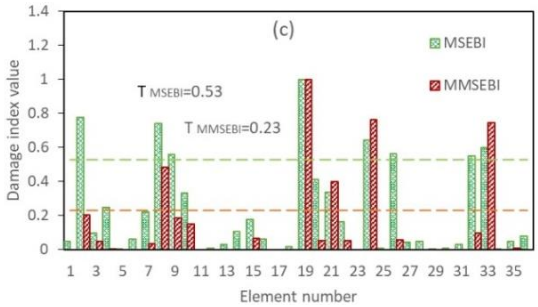

(c) Scenario 3 (damaged elements: 19, 24)

Fig. 23 The normalized MSEBI and MMSEBI comparison for the 36-bar spatial truss for sensor pattern 2 considering 5 modes with 3% noise

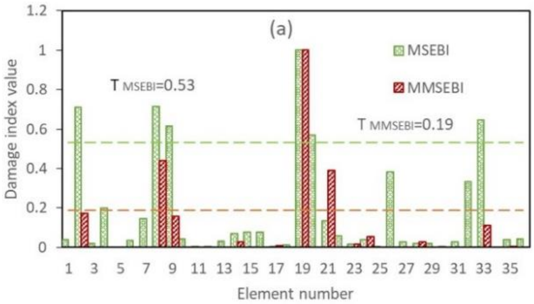

(a) Scenario 1 (damaged element: 19)

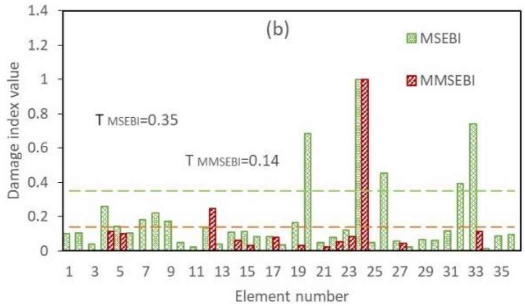

(b) Scenario 2 (damaged element: 24)

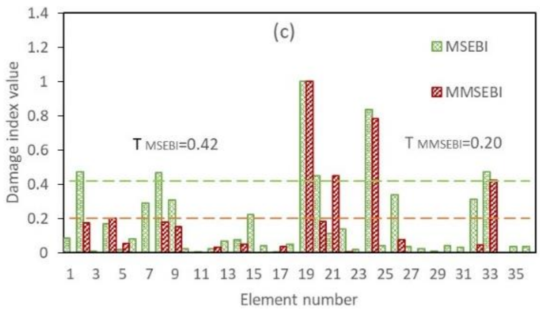

(c) Scenario 3 (damaged elements: 19, 24)

Fig. 24 The normalized MSEBI and MMSEBI comparison for the 36-bar spatial truss for sensor pattern 2 considering 7 modes with 3% noise

when 5 modes and 3% noise are considered. For the first damage scenario as shown in the figure, the MSEBI has some errors. In addition to damaged element 19, other healthy elements such as 8, 9 and 32 have also been wrongly detected. In contrast, the MMSEBI has been correctly identified damaged element 19 by detecting healthy elements 8, 9 and 21 as damaged elements. In the second damage scenario, the MSEBI incorrectly recognized three healthy elements including 2, 8 and 9 as damaged elements. Though, the MMSEBI has identified only two elements 5 and 12 in addition to the damaged elements. In the third scenario, more errors are achieved by MSEBI. The healthy elements 2, 8, 9, 26, 32 and 33 are incorrectly diagnosed as damaged elements, implying that MSEBI

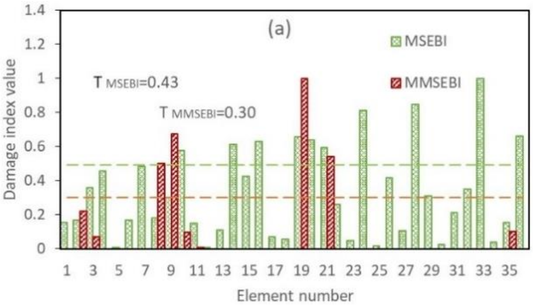

(a) Scenario 1 (damaged element: 19)

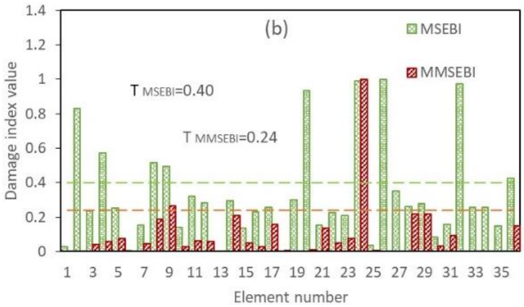

(b) Scenario 2 (damaged element: 24)

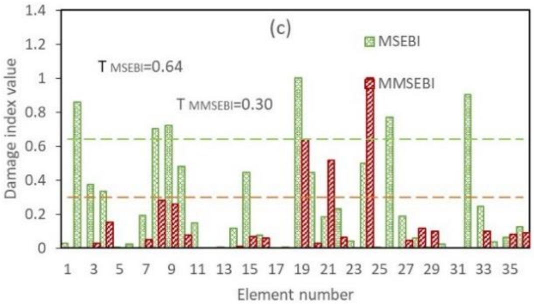

(c) Scenario 3 (damaged elements: 19, 24)

Fig. 25 The normalized MSEBI and MMSEBI comparison for the 36-bar spatial truss for sensor pattern 2 considering 5 modes with 7% noise

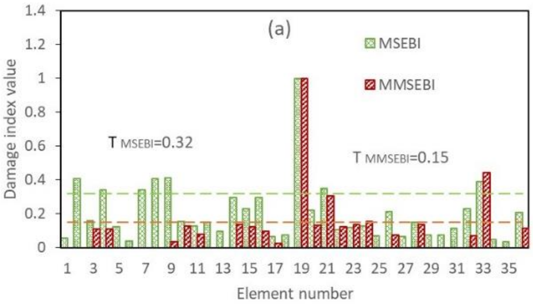

(a) Scenario 1 (damaged element: 19)

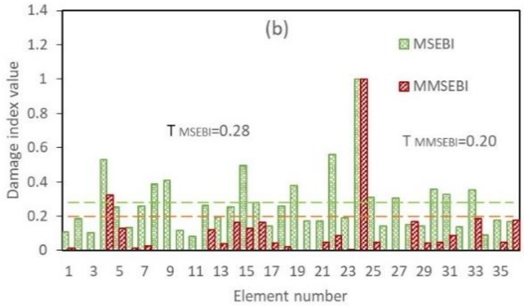

(b) Scenario 2 (damaged element: 24)

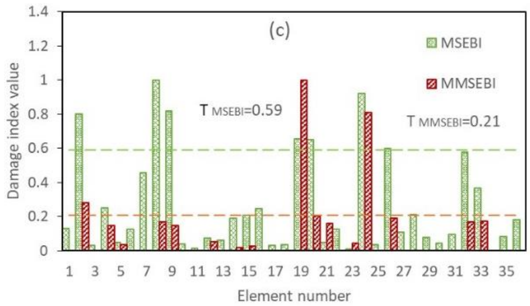

(c) Scenario 3 (damaged elements: 19, 24)

Fig. 26 The normalized MSEBI and MMSEBI comparison for the 36-bar spatial truss for sensor pattern 2 considering 7 modes with 7% noise

index has lost its efficacy.

In contrast, MMSEBI has delivered higher correct damage identification rate and merely the index value for elements 8, 21 and 33 is unfavorable. Thus, the suggested index has a better competence compared with MSEBI.

For evaluating the effect of mode numbers, the results of MSEBI and MMSEBI are presented. Fig. 24 reveals the normalized MSEBI and MMSEBI values for the second pattern of master DOFs for considering 7 modes with 3% noise. It can be observed that the MMSEBI considering 7 modes can correctly identify the damage location for all damage scenarios, only one false element in the second scenario and two false elements in the first and third scenarios are achieved, which it indicates the performance of the proposed index.

Fig. 25 shows the normalized MSEBI and MMSEBI values for the second pattern of master DOFs when 5 modes and 7% noise are considered. From the results in the figure, for the first damage scenario, the MSEBI contains many false elements. In addition to the damaged element 19 identified, other elements such as 10, 14, 16, 20, 21, 24, 26, 28, 33 and 36 have also been wrongly detected. In fact, in this pattern the indicator has lost its efficiency. Moreover, the damaged element 19 has been properly identified with three false elements (8, 9 and 21) by MMSEBI. For the second scenario, the MSEBI recognized damaged element 24 correctly but high healthy elements including 2, 4, 8, 9, 20 26, 32 and 36 are identified as damaged elements. While, the MMSEBI has identified the damaged elements and just one element (9) has been incorrectly detected, which it shows the high efficiency of the index. In the third damage scenario, the MSEBI has been led to a greater error and the elements 2, 8, 9, 26 and 32 are wrongly recognized as damaged elements. Moreover, the damage locations have been properly identified with one error (element 21) by MMSEBI. Consequently, it can be said that the modified index has a better capability for damage identification even by increasing the noise level compared with the previous index.

The normalized MSEBI and MMSEBI values are shown in Fig. 26 for considering 7 modes via 7% noise. It can be seen that the MMSEBI considering 7 modes can correctly identify the damage location for all damage scenarios with only one or two false elements, which it indicates the performance of the proposed index even by increasing the noise level.

A result summary of damage identification obtained by MSEBI and MMSEBI without considering noise are provided in Table 8. As can be seen, the MSEBI and MMSEBI have the similar performance in detecting damaged elements for damage scenarios 1, 2 and 3.

Table 9 summarizes the damage identification results obtained by MSEBI and MMSEBI, considering 3% of noise. As shown, the MSEBI contains a lot of errors in detecting the damaged element in scenarios 1, 2 and 3. The MMSEBI is falsely detected only one or two elements as the damaged element in the scenarios 1, 2 and 3 and three elements when 7 modes are considered. It can be observed that by increasing the number of modes to 7, the efficiency of MMSEBI for damage identification has been enhanced.

Table 10 reports a summary of damage identification results obtained by MSEBI and MMSEBI with 7% of noise. As shown, the MSEBI contains a lot of errors in detecting the damaged element in scenarios 1, 2 and 3. Moreover, the MMSEBI is falsely detected only one or two elements as the damaged element in all damage scenarios when 7 modes are considered. It can be observed that by increasing the number of modes to 7, the efficiency of MMSEBI for damage identification has been improved, however, the increase in the number of modes has a little effect on the performance of the MSEBI index.

Moreover, for the MSEBI, the first pattern of DOFs has a better efficiency compared with the second pattern of DOFs. Though, in both patterns, a great deal of error has been gained. However, the use of the MMSEBI has resulted in a good performance in both damage patterns which damaged elements are properly identified. Both patterns have rather the same efficiency for damage identification.

Table 8 Damage elements identified for the 36-bar spatial truss without considering noise

Scenarios	MDOF Pattern	Actual damage	3 modes		4 modes	
			MSEBI	MMSEBI	MSEBI	MMSEBI
Scenario1	MDOF Pattern 1	19	19	19	19	19
Scenario2		24	24	24	24	24
Scenario3		19, 24	19, 24	19, 24	19, 24	19, 24
Scenario1	MDOF Pattern 2	19	19	19	19	19
Scenario2		24	24	24	24	24
Scenario3		19, 24	19, 24	19, 24	19, 24	19, 24

Table 9 Damage elements identified for the 36-bar spatial truss with considering 3% noise

Scenarios	MDOF Pattern	Actual damage	5 modes		7 modes	
			MSEBI	MMSEBI	MSEBI	MMSEBI
Scenario1	MDOF Pattern 1	19	3, 10, 11, 19, 30	10, 11, 19, 30	10, 11, 19, 30	10, 19
Scenario2		24	1, 14, 24, 33	24, 33	3, 10, 24	3, 24
Scenario3		19, 24	3, 10, 19	3, 19, 24, 30	3, 10, 11, 19, 24	19, 24
Scenario1	MDOF Pattern 2	19	8, 9, 19, 32	8, 9, 19, 21	2, 8, 9, 19, 20, 33	8, 19, 21
Scenario2		24	2, 8, 9, 24	5, 12, 24	20, 24, 26, 32, 33	12, 24
Scenario3		19, 24	2, 8, 9, 19, 24, 26, 32, 33	8, 19, 21, 24, 33	2, 8, 19, 20, 24, 33	19, 21, 24, 33

Table 10 Damage elements identified for the 36-bar spatial truss with considering 7 % noise

Scenarios	MDOF Pattern	Actual damage	5 modes		7 modes	
			MSEBI	MMSEBI	MSEBI	MMSEBI
Scenario1	MDOF Pattern 1	19	1, 10, 11, 19, 25, 30	10, 11, 19, 30	3, 10, 11, 13, 15, 19	10, 11, 19
Scenario2		24	1, 3, 10, 11, 13, 14, 20, 22, 33	13, 24, 33	3, 10, 11, 22, 24	22, 24
Scenario3		19, 24	10, 11, 15, 19, 24, 30	19, 24, 25, 30	10, 11, 15, 19, 24	19, 22, 24
Scenario1	MDOF Pattern 2	19	10, 14, 16, 19, 20, 21, 24, 28, 33, 36	8, 9, 19, 21	2, 4, 7, 8, 9, 19, 21, 33	19, 21, 33
Scenario2		24	2, 4, 8, 9, 20, 24, 26, 32, 36	9, 24	4, 8, 9, 15, 19, 22, 24, 25, 27, 28, 30, 33	4, 24
Scenario3		19, 24	2, 8, 9, 19, 26, 32	19, 21, 24	2, 8, 9, 19, 20, 24, 26	2, 19, 24

6. Conclusions

The aim of this paper is to introduce an efficient index for identifying structural damage when the response exists in a limited number of degrees of freedom. Moreover, the proposed method is based on the reconstruction of mode shapes using Improved Reduction System (IRS) method. First, the IRS method has been employed to estimate the slave DOF responses using the master DOF responses and then, based on all DOFs, a damage index named as MMSEBI has been proposed. Two numerical examples including a planar frame and a 3D truss, were employed to evaluate the effectiveness of the proposed index and a parametric study considering mode numbers, noise effect, and sensor pattern has been made. Also, the performance of the proposed index MMSEBI has been compared with that of the available index MSEBI. The obtained modal strain energy based index has been normalized and the universal threshold based on statistical hypothesis testing principles has been applied for damage index values. According to the outcomes, the proposed MMSEBI index had better performance as compared with MSEBI for recognizing the actual location of the damage especially when the noise level has been considered. Furthermore, by increasing the number of modes, the proposed MMSEBI index has a better performance, being able to identify damaged location correctly. Moreover, it should be noted that the efficiency of MMSEBI for damage identification is superior to the MSEBI while its threshold is greater. Numerical results indicate that the combination of MMSEBI and IRS method can provide a reliable tool to identify the location of damage accurately.

References

Alves, M., Yu, J. and Jones, N. (2000), “On the elastic modulus degradation in continuum damage mechanics”, *Comput. Struct.*, **76**(6), 703-712. https://doi.org/10.1016/S0045-7949(99)00187-X

Asgarian, B., Amiri, M. and Ghafooripour, A. (2009), “Damage detection in jacket type offshore platforms using modal strain energy”, *Struct. Eng. Mech., Int. J.*, **33**(3), 325-337. https://doi.org/10.12989/sem.2009.33.3.325

Ashory, M.R., Ghasemi-Ghalebahman, A. and Kokabi, M.J. (2018), “An efficient modal strain energy-based damage detection for laminated composite plates”, *Adv. Compos. Mater.*, **27**(2), 147-162. https://doi.org/10.1080/09243046.2017.1301069

Ding Q., Zou, C., Tang, Y. and Zhang, S. (2013), “Damage detection in road and bridge based on modal strain energy method”, *Proceedings of the 4th International Conference on Transportation Engineering* (*ICTE 2013*), Chengdu, China, pp. 1753-1758.

Dinh-Cong, D., Vo-Duy, T., Ho-Huu, V., Dang-Trung, H. and Nguyen-Thoi, T. (2017), “An efficient multi-stage optimization approach for damage detection in plate structures”, *Adv. Eng. Softw.*, **112**, 76-87. https://doi.org/10.1016/j.advengsoft.2017.06.015

Dongyu, X., Cheng, X., Shifeng, H. and Minhua, J. (2010), “Identifying technology for structural damage based on the impedance analysis of piezoelectric sensor”, *Constr. Build. Mater.*, **24**(12), 2522-2527. https://doi.org/10.1016/j.conbuildmat.2010.06.004

Guan, H. and Karbhari, M. (2008), “Improved Damage Detection Method Based on Element Modal Strain Damage Index Using Sparse Measurement”, *J. Sound Vib.*, **309**(3), 465-494. https://doi.org/10.1016/j.jsv.2007.07.060

Guo, H.Y. and Li, Z.L. (2009), “A two-stage method to identify structural damage sites and extents by using evidence theory and micro-search genetic algorithm”, *Mech. Syst. Sig. Process.*, **23**(3), 769-782. https://doi.org/10.1016/j.ymssp.2008.07.008

Guyan, R.J. (1985), “Reduction of stiffness and mass matrices”, *AIAA Journal*, **3**(2), 380-380. https://doi.org/10.2514/3.2874

Hu, H. and Wu, C. (2009), “Development of scanning Damage Index for the Damage Detection of Plate Structures using Modal strain Energy Method”, *Mech. Syst. Sig. Process.*, **23**(2), 274-287. https://doi.org/10.1016/j.ymssp.2008.05.001

Janeliukstis, R., Rucevskis, S., Wesolowski, M. and Chate, A. (2017), “Damage identification in beam structure based on thresholded variance of normalized wavelet scalogram”, *IOP Conference Series*, *3rd International Conference on Innovative Materials*, *Structures and Technologies* (*IMST 2017*), Riga, Latvia, September.

Kaveh, A., Javadi, S.M. and Maniat, M. (2014), “Damage assessment via modal data with a mixed particle swarm strategy, Ray optimizer, and Harmony search”, *Asian J. Civil Eng.* (*BHRC*), **15**(1), 95-106.

Kim, J.T., Ryu, Y.S., Cho, H.M. and Stubbs, N. (2003), “Damage identification in beam-type structures: frequency-based method vs mode-shape-based method”, *Eng. Struct.*, **25**(1), 57-67. https://doi.org/10.1016/S0141-0296(02)00118-9

Li, P., Zhu, H., Hui, L. and Shun, W. (2015), “Structural damage identification based on genetically trained ANNs in beams”, *Smart Struct. Syst., Int. J.*, **15**(1), 227-244. https://doi.org/10.12989/sss.2015.15.1.227

Li, Y., Wang, S., Zhang, M. and Zheng, C. (2016), “An Improved Modal Strain Energy Method for Damage Detection in Offshore

Platform Structures", *J. Mar. Sci. Appl.*, **15**(2), 182-192. https://doi.org/10.1007/s11804-016-1350-1

Liu, F., Li, H., Li, W. and Wang, B. (2014), "Experimental study of improved modal strain energy method for damage localization in jacket-type offshore wind turbines", *Renew. Energy*., **72**, 174-181. https://doi.org/10.1016/j.renene.2014.07.007

Moradipour, P., Chan, T.H.T. and Gallage, C. (2015), "An improved modal strain energy method for structural damage detection, 2D simulation", *Struct. Eng. Mech., Int. J.*, **54**(1), 105-119. https://doi.org/10.12989/sem.2015.54.1.105

Nguyen, K.D., Chan, T.H.T. and Thambiratnam, D.P. (2016), "Structural damage identification based on change in geometric modal strain energy-eigenvalue ratio", *Smart Mater. Struct.*, **25**(7), 075032. https://doi.org/10.1088/0964-1726/25/7/075032

O'Callahan J.C. (1989), "A procedure for an Improved Reduced System (IRS) model", *Proceedings of the 7th International Modal Analysis Conference* (*IMAC 1989*), Las Vegas, NV, USA, pp. 17-21.

Seyedpoor, S.M. (2012), "A two stage method for structural damage detection using modal strain energy based index and particle swarm optimization", *Int. J. Non Linear Mech.*, **47**(1), 1-8. https://doi.org/10.1016/j.ijnonlinmec.2011.07.011

Seyedpoor, S.M. and Montazer, M. (2016), "A two-stage damage detection method for truss structures using a modal residual based indicator and differential evolution algorithm", *Smart Struct. Syst., Int. J.*, **17**(2), 347-361. https://doi.org/10.12989/sss.2016.17.2.347

Shi, Z.Y., Law, S.S. and Zhang, L.M. (1998), "Structural damage localization from modal strain energy change'', *J. Sound Vib.*, **218**(5), 825-844. https://doi.org/10.1006/jsvi.1998.1878

Shi, Z.Y., Law, S.S. and Zhang, L.M. (2000a), "Structural damage detection from modal strain energy change", *J. Eng. Mech.*, **126**(12), 1216-1223. https://doi.org/10.1061/(ASCE)0733-9399(2000)126:12(1216)

Shi, Z.Y., Law, S.S. and Zhang, L.M. (2000b), "Damage localization by directly using incomplete mode shapes", *J. Eng. Mech.*, **126**(6), 656-660. https://doi.org/10.1061/(ASCE)0733-9399(2000)126:6(656)

Shi, Z.Y., Law, S.S. and Zhang, L.M. (2002), "Improved damage quantification from elemental modal strain energy change", *J. Eng. Mech.*, **128**(5), 521-529. https://doi.org/10.1061/(ASCE)0733-9399(2002)128:5(521)

Shih, H.W., Thambiratnam, D.P. and Chan, T.H.T. (2009), "Vibration based structural damage detection in flexural members using multi-criteria approach", *J. Sound Vib.*, **323**(3-5), 645-661. https://doi.org/10.1016/j.jsv.2009.01.019

Stubbs, N., Kim, J.T. and Topole, K. (1992), "An efficient and robust algorithm for damage localization in offshore platforms", *Proceedings of the 10th ASCE Structures Congress*, USA, March, pp. 543-546.

Stubbs, N., Kim, J.T. and Farrar, C.R. (1995), "Field verification of a non-destructive damage localization and severity estimation algorithm", *Proceedings of the 13th International Modal Analysis Conference* (*IMAC 1995*), USA, pp. 210-218.

Tan, Z.X., Thambiratnam, D.P., Chan, T.H.T. and Abdul Razak, H. (2017), "Detecting damage in steel beams using modal strain energy based damage index and Artificial Neural Network", *Eng. Fail. Anal.*, **79**, 253-262. https://doi.org/10.1016/j.engfailanal.2017.04.035

Wahalthantri, B.L., Thambiratnam, D.P., Chan, T.H.T. and Fawzia, S. (2012), "An Improved method to detect damage using modal strain energy based damage index", *Adv. Struct. Eng.*, **15**(5), 727-742. https://doi.org/10.1260/1369-4332.15.5.727

Wang, F.L., Chan, T.H.T., Thambiratnam, D.P. and Tan, A.C.C. (2010), "Damage detection for truss bridge structures using correlation-based structural modal strain energy", *The Proceedings of the 8th International Conference on Short and Medium Span Bridges*, Nia-gara Falls, ON, Canada, August.

Wang, S., Zhang, M. and Liu, F. (2013), "Estimation of semi-rigid joints by cross modal strain energy method", *Struct. Eng. Mech., Int. J.*, **47**(6), 757-771. https://doi.org/10.12989/sem.2013.47.6.757

Wu, S., Zhou, J., Rui, S. and Fei, Q. (2016), "Reformulation of elemental modal strain energy method based on strain modes for structural damage detection", *Adv. Struct. Eng.*, **20**(6), 896-905. https://doi.org/10.1177/1369433216665626

Yan, W.J., Ren, W.X. and Huang, T.L. (2012), "Statistic structural damage detection based on the closed-form of element modal strain energy sensitivity", *Mech. Syst. Signal Process.*, **28**, 183-194. https://doi.org/10.1016/j.ymssp.2011.04.011

Yazdanpanah, O., Seyedpoor, S.M. and Bengar, H.A. (2015). "A new damage detection indicator for beams based on mode shape data", *Struct. Eng. Mech., Int. J.*, **53**(4), 725-744. https://doi.org/10.12989/sem.2015.53.4.725.

CC